UNIVERSITY OF CALIFORNIA, SAN DIEGO

Effects of Fiber Type and Manufacturing Process on the Mechanical Properties of Natural Fiber Composite Fiberboard

A Thesis submitted in partial satisfaction of the requirements
for the degree Master of Science

in

Structural Engineering

by

Winnie Elva Ding

Committee in charge:

Professor Hyonny Kim, Chair
Professor Francesco Lanza Di Scalea
Professor Qiang Zhu

2014

The Thesis of Winnie Elva Ding is approved, and it is acceptable in quality and form for publication on microfilm and electronically:

Chair

University of California, San Diego

2014

TABLE OF CONTENTS

LIST OF ABBREVIATIONS

FPL: Forest Products Lab

HP: high performance panels, with resin coating

MDF: medium-density fiberboard

NET: Noble Environmental Technologies

OCC: recycled old corrugated cardboard

RA: raw panels, as manufactured, not coated with resin

RT: RockTenn, an externally sourced recycled fiberboard tested in this study

VOC: volatile organic compound

WL: wet lap, recycled office paper

LIST OF FIGURES

LIST OF TABLES

ACKNOWLEDGEMENTS

I would like to acknowledge Professor Hyonny Kim for providing me the opportunity to join his lab and for his guidance and support as my advisor and chair of my committee. I would also like to thank Dr. Jen Rhymer at Noble Environmental Technologies (NET) for all her contributions and, along with the rest of the team at NET, for allowing me the opportunity to intern at NET and investigate ECOR®. My fellow lab members have been invaluable in showing me how to operate various tools and devices used during my time on this project. I would like to also acknowledge Professor Lanza di Scalea and Professor Qiang Zhu for participating on my thesis committee.

ABSTRACT OF THE THESIS

Effects of Fiber Type and Manufacturing Process on the Mechanical Properties of Natural Fiber Composite Fiberboard

by

Winnie Elva Ding

Master of Science

University of California, San Diego, 2013

Professor Hyonny Kim, Chair

ECOR®, a product of Noble Environmental Technologies, is a sustainable alternative to tradition wood panels and fiberboard products. ECOR® panels are made by hot pressing wet fiber pulp of urban and agricultural fibers, such as recycled corrugated cardboard, recycled office paper, kenaf core fibers, oat, or a mix of cardboard with one alternate fiber. This project studies the performance of raw (RA) panels, which are as-manufactured without resin coating, and high performance (HP) panels. HP panels were made by applying Entropy SuperSap resin in varying viscosity mixes to panels that had been desiccated at 150°C (302°F) for 30 min. Variations on resin application methodology and curing conditions were tested, but none resulted in full infusion of resin

through the panel thickness. Tensile and short beam shear tests were performed on specimens of varying fiber content and panel density. Tensile and shear strengths of raw panels were found to increase roughly linearly with density. More highly processed urban fiber panels such as corrugated cardboard and office paper showed stronger properties than the less processed and often stiffer, lignin-coated agricultural fiber panels, such as kenaf and oat. The strength of HP panels increases compared to their RA counterparts but the amount of increase levels off with increasing density, possibly limited by the strength of the resin itself. The application of lower viscosity resin results in higher strength HP panels than resins with higher viscosity, suggesting more effective infusion of the lower viscosity resin into the voids of the fiber panels.

.

1 INTRODUCTION

This project has been developed in conjunction with the San Diego, CA based company Noble Environmental Technologies (NET). NET is interested in further development of their product ECOR®, a fiberboard material made from natural, often recycled fibers. This section describes NET and ECOR®, highlights the motivation and importance of the work, and defines the objectives for the project.

NET is a clean technology and manufacturing company incorporated in 1992 to develop and commercialize the product ECOR®, first developed by Forest Products Lab (FPL) in the U.S. Division of Agriculture [1]. The panels are 100% bio-based, and the process does not involve the use of any volatile organic compounds (VOCs) or waste products other than water. NET provides raw material manufacturing as well as design services for products using ECOR® panels. The panels are currently used for various interior applications including movie stages and sets, furniture, signage, room partitions, packaging, and more. ECOR® is formed from readily available urban waste fiber (e.g., post-consumer paper and cardboard products) and agricultural waste (e.g., treetop forest residue). It is a relatively strong, lightweight material, suitable as an alternative for typical materials such as particleboard, plywood, medium density fiberboard (MDF), aluminum, and plastic.

1.1 MOTIVATION

Growing concern over the depletion of natural resources and heightened environmental awareness have prompted a shift toward the use of renewable materials

with lower embodied energy than traditionally used in construction and product design. Though the resources of the world may have appeared vast in the past, industrial consumption has grown so large that the limited nature of our resources cannot be ignored. In addition to taxing limited resources, traditional materials often require a high input energy to process and manufacture. Metals especially carry a high embodied energy, requiring extremely high energy for making the base materials, often from mined ores, and high temperatures for heat treatment, melting, or making workable. Both the use of raw resources and the consumption of energy are costly, providing economic as well as environmental motivation for minimizing the use of newly-made materials.

Many materials traditionally used in construction and a variety of consumer products contain chemicals known as VOCs, which off-gas harmful fumes into the air. If these materials are stored indoors, this causes a buildup of VOCs that contributes significantly to poor indoor air quality and is linked to a range of illnesses. Many resins used in fiber-reinforced plastic composite materials exhibit high levels of VOCs, posing health risks to consumers. In addition to health concerns, the combination of resin with natural fiber material (common in the field of available natural composites) is generally not a reversible process, preventing effective recycling of the plastic, the fibers, or both. With our limited resources, the ability to give old material a new life-cycle is desirable. Full recyclability is possible of a purely fiber-based material but only if resin has not been mixed into the fibers. Creating high value materials out of end-of-life urban materials and agricultural waste materials has the additional benefit of keeping these materials out of the landfill. In the case of residual forest trimmings, the material is often

left to decompose on forest floor, increasing the fuel load for forest fires [2]. Using the material for fiberboard production reduces the fire hazard from residual trimmings.

Agricultural waste and post-consumer recyclables can be used in the production of fiberboards, turning a waste material into high value material with various industrial applications. These fiberboards require minimal processing energy to produce and are entirely derived of natural fibers, minimizing harmful chemical exposure and promoting a cradle-to-cradle industry of reuse rather than waste. Requiring only simple and low energy processing equipment, the factories can be situated locally, minimizing shipping footprint between agricultural waste and production facilities.

In order to become standard and commonly used materials, sustainable materials must demonstrate consistency and properties that are comparable to those being replaced. A comprehensive understanding of factors affecting various properties, most importantly strength and water-resistance, is therefore of interest.

More specific to NET, future directions and goals of the company strongly affect the goals of this study. Currently, the ECOR® line of fiberboards is primarily based on old corrugated cardboard (OCC) and wet lap (WL) pulped office paper fibers. In addition to using post-consumer recyclables, it is also of interest to develop panels incorporating agricultural waste fibers, thereby achieving high value products out of an otherwise low value, problematic material. However, different fiber properties affect the resultant panel properties significantly. Currently, to test the suitability of new fiber sources, a large enough sample of the fibers must be obtained and formed into panels in

the factory. The ability to predict the suitability of new fiber sources without resorting to trial-and-error would be of use in developing new fiber blends.

In this study, mechanical testing is performed on panels comprised of a selection of fiber types and fiber combinations, and pressed at varying pressures, to determine the corresponding material properties. These pure fiber panels without additives are known as raw (RA) panels. A more comprehensive and systematically determined set of material properties will result, refining the currently reported values. The resulting information is synthesized with published knowledge to understand the link between fiber properties or panel manufacturing parameters and resultant panel properties. Understanding of this relation will contribute greatly to the assessment of new potential fiber types.

Another future direction in the development of ECOR® is obtaining higher strengths and water-resistance by infusing the panels with an eco-friendly resin, for a line of high performance (HP) panels. Preliminary efforts are explored using SuperSap Resin (Entropy Resins, Inc., Hayward, CA), a partially bio-based resin.

1.2 OBJECTIVES

The objectives of this project are to:

- assess strength properties for varying panel fiber compositions, panel densities, and resin applications,
- understand how strength properties are affected by fiber type and panel density,

- explore methods of resin infusion, and
- measure the effect of resin-infusion/coating on properties and compare with uncoated base panels.

2 LITERATURE REVIEW

2.1 FIBER MORPHOLOGY AND EXTRACTION

Natural fibers can be derived from both animal and plant sources; the focus of this project is specifically on plant fibers, which consist primarily of cellulose, hemicellulose, and lignin. Less homogeneous than wood, annual plants also have a waxy epidermis composed of inorganic substances like ash and silica in addition to cellulose and lignin [3]. Cellulose is a hydrophilic semi-crystalline polymer that forms a linear chain containing alcoholic hydroxyl groups. These hydroxyl groups form inter- and intramolecular hydrogen bonds. The length of polymer chains varies for different fibers, and longer chains generally correlate to higher strength properties [4]. The majority of plant-based cellulose has a high packing density, forming crystalline regions of cellulose [5]. Compared to cystalline regions, the less densely packed amorphous regions of cellulose microfibrils exhibit less hydrogen bonding with adjacent cellulose chains and are thus more available to bond with water vapor in the air [6].

Hemicellulose is a branched polymer consisting of repeating sugar molecules. Unlike cellulose, hemicellulose composition varies between plant species and crops. It is amorphous and very hydrophilic [6]. The degree of polymerization, relating directly to the length of polymer chains, is lower than in cellulose fibers, resulting also in lower strengths [7]. Hemiceulluloses, along with lignin, form a supporting matrix around the cellulose microfibrils, adhering to the cellulose through hydrogen bonding [6].

Lignin is a biochemical polymer that fills in the spaces between cellulose and hemicellulose components, and provides rigidity and structural support within the plant by forming crosslinks between hydroxyls in the lignin and hydroxyls in the cellulose. Lignin is amorphous and hydrophobic. It can also be used as a thermoplastic polymer, with a glass transition temperature around 90°C and a melting point around 170°C [6].

Plant fibers consist of layers of cell walls surrounding a center lumen, with the cell walls being composed of oriented cellulose microfibrils embedded in a hemicellulose/lignin matrix, as shown in Figure 1. Different plants vary in the ratios of cellulose, hemicellulose, and lignin, as well as the orientation of the cellulose. The angle between cellulose microfibrils and the fiber axis is known as the microfibrillar angle, which affects the stiffness and strength of the fibers. When the microfibrils are nearly parallel to the fiber axis (between 7° and 12°), the fibers exhibit higher strength, while fibers with spiraled cellulose chains, closer to 30° from the fiber axis, exhibit much lower tensile strengths [7].

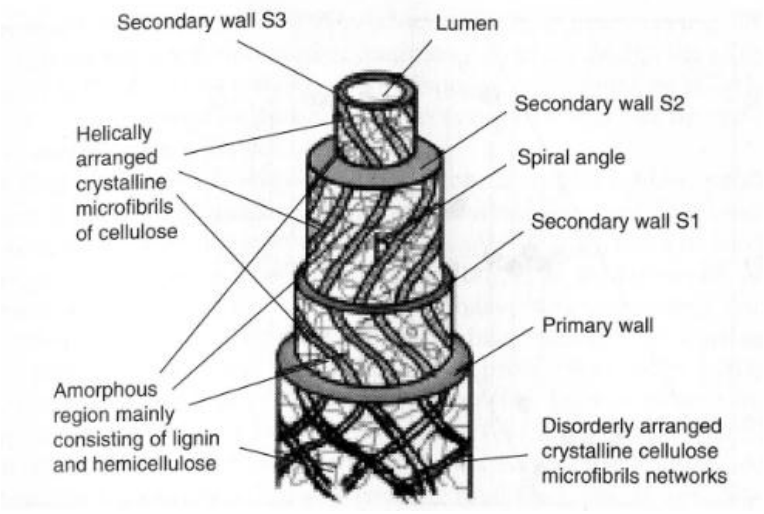

Figure 1: Structure of a plant fiber showing cell walls and spiraled fibers around the lumen [6].

When fibers with spiraled cellulose are under tension, either the microfibrils start to despiral or they elongate toward the noncrystalline regions. Analysis of fibers also suggests correlation between larger spiral angles and lower cellulose content [8]. Another physical characteristic with significant impact on strengths properties is the aspect ratio or slenderness ratio, L/D, defined as the fiber length over fiber diameter. Higher ratios correlate to higher surface area to per unit volume and thus better fiber-fiber bonding, thereby leading to higher properties [9].

The lignin bonding fibers together must be broken to free individual fibers for use in fiberboard production. A common method for fiber extraction is called refining, a process in which the material is pressed through a gap between two rotating disks with radial grooves, forcing fibers and fiber bundles apart. Steaming or applying chemical treatments before passing the material through the refiner can weaken the lignin bonds, allowing the cellulose fibers to pull apart more easily and with less damage. The amount of output fiber, or yield, is lower when steam or chemical treatment is applied because more of the lignin material is removed, but the fibers that result are of higher quality [10].

2.2 Natural Fiber Composites

Natural fiber composites commonly consist of a resin matrix reinforced with natural fibers. Fiberboards utilize the inherent long-fiber structure in plants, while particleboards use the fibers in particle form such as sawdust or powdered annual plant waste material. Particleboards are made using a dry process in which the particles are randomized and distributed by airflow, and then pressed into panel form, typically with a heat-activated adhesive. Often the faces of the panel are composed of finer particles than

the core for a smoother surface suitable for overlaying or veneering [11]. Fiberboards can be made with dry or wet processes. Fibers are coated with adhesives and pressed into a mat to form dry-process fiberboards [12]. Wet-process fiberboards involve a pulp of fibers in water that is then drained and pressed. When a polymer matrix is used to hold the fibers together, significant challenges arise in the fiber-matrix interfacial bonding due to a mismatch in surface polarity between the hydrophilic biological fibers and the hydrophobic polymers, weakening the strength of the overall composite.

As an alternative, binderless fiberboards such as ECOR® have been developed, which rely on autoadhesion between fibers instead of an added resin matrix. Water is used to form a fiber pulp over a mesh screen, then the water is allowed to flow through the screen before the remaining fibers are heated and pressed [12].

Published studies from previous work on binderless fiber composites can provide important insights on fiber characteristics, treatments, or processing techniques which affect panel properties. One method for forming fiberboard panels uses lignin as a natural thermoplastic binding agent. When lignin is heated in water above its glass transition temperature, the lignin softens. This is suspected to occur as intermolecular hydrogen bonds within the lignin are replaced by hydrogen bonds between lignin and water [13]. It is hypothesized that fibers with lignin-rich surfaces become bonded under pressure as the softened lignin molecules mechanically entangle and potentially form covalent bonds with each other [14]. However, variation across plant types, regions, and treatment processes causes unpredictable polymerization characteristics [15].

A different approach, used for ECOR® panels, relies on bonding between cellulose fibers without the use of lignin as an adhesive. Studies from FPL, the developers of the method used for ECOR® panels, show that increased levels of fiber refinement improves bonding between fibers. However, more refining (extra passes through the refiner and/or a smaller gap width between disks) cuts down on resulting fiber lengths, which can be detrimental to overall strength. Shorter fibers also slows the rate of water drainage and thereby slows production time. Addition of NaOH solution in the separation process softens the lignin, allowing for separation of cellulose with less damage, resulting in longer fiber lengths as fewer fibers are broken during separation, while improving entanglement and drainage speed [1].

Fibers are flexible and form bonded substructures as they come in contact with each other and entangle. During pulping and slushing, the fibers are in a shear field causing them to bend, fold, and rotate. When the motion ceases, fibers are spatially inhibited from straightening out and come to rest in a pre-strained state [16]. Though the natural fibers are relatively strong, when pressed into fiberboard panels the main weakness in properties tends to be due to the fiber-fiber bonding rather than the individual fiber strengths [17].

Processing of raw plant materials for paper and fiberboard production often aims to isolate the cellulose fibers and remove as much lignin as possible from the fiber surfaces through a variety of mechanical and chemical fiber extraction methods. Residual lignin on the fibers increases stiffness of the fibers, reducing their ability to fold and entangle [18]. Fewer bonding sites between fibers results in a lower overall panel

strength. Hunt and Supan [10] with FPL have shown that removal of lignin, which occurs for highly treated fibers such as corrugated cardboard fibers, results in more flexible and bondable fibers. This flexibility allows the fibers to conform intimately with each other, resulting in a higher degree of fiber-fiber bonding and producing a denser panel [10].

Variations in tensile strength have been shown to depend strongly on fiber lengths and cell wall thickness. Bark fibers tend to produce long, slender fibers having higher performance, while core fibers are shorter and thicker, reducing fiber surface area contact and therefore reducing potential locations for interfiber bonding [9].

From this review, the mechanical properties of fiberboard and natural fiber composites are clearly affected by the source of fiber material and how the fibers are processed. Fiber sourcing and processing affect the fiber lengths, resulting bonding surface area, and fiber flexibility, which in turn affect the properties of resulting fiberboards. An understanding of which fiber characteristics are most influential and whether panel formation processes have more impact on panel properties than the inherent fiber properties could be of great use to fiberboard manufacturers looking to use a variety of fiber sources. Such an understanding could allow manufacturers to determine the suitability of new fiber types for use in fiberboards without the need to determine all of the fiber characteristics, nor having to make a trial panel of the new fiber type.

3 EXPERIMENTAL SETUP

3.1 ECOR® PANEL PREPARATION

For the production of ECOR®, fiber is pulped in a fiber-water solution with concentrations below 6% fiber volume fraction. Because of the low density of fibers and since the suspension has a high percentage of water, the fibers float horizontally so that the resulting panels are composed of fibers primarily lying in the plane of the panel (i.e., single horizontal plane defined by free surface). The water is drained out of the fiber suspension with suction, heat and pressure. The bed of the press is heated to 176.7°C (350°F) and pressed at 50, 100, or 150 psi, for about 10 min when very little moisture content is left. The resulting panels have an average thickness of 2.54 mm. While exact density varies by fiber type, the 150 and 250 psi pressures produced panels of roughly 18% and 33% higher density relative to the 50 psi panels, respectively.

The standard panels are comprised of pulped old corrugated cardboard (OCC) or recycled white office paper pulp, known as wet lap (WL). ECOR® panels included in this study are manufactured with differing blends of recycled urban, forest, or agricultural materials. Panel materials in the urban set include:

- Old corrugated cardboard (OCC)
- Wet Lap (WL), recycled white office paper
- RockTenn (RT), a pulp of mixed recycled products.

Materials in the agricultural category include:

- Kenaf fiber
- Oat.

Several blended fiberboards were studied, including

- 25% OCC and 75% WL (referred to as 25/75 OCC/WL)
- 50% OCC and 50% WL (referred to as 50/50 OCC/WL)
- 50% OCC and 50% kenaf (referred to as 50/50 OCC/Kenaf)
- 50% OCC and 50% oat (referred to as 50/50 OCC/Oat)
- 75% OCC and 25% kenaf (referred to as 75/25 OCC/Kenaf)
- 75% OCC and 25% oat. (referred to as 75/25 OCC/Oat)

OCC, WL, and RT fibers are all recycled urban fibers, and thus have been processed and refined more than the agricultural series of fibers. Oat does not bind together well, crumbling easily if pressed in a 100% oat panel, but can be blended with OCC for a stronger average panel. Note that RT is an externally sourced book board material, produced differently than the typical ECOR® panel. The kenaf fibers used are shorter core fibers, a waste product from Kelly Paper, which extracts the longer kenaf bark fibers for paper products. To highlight the variation between fiber types, microscope images were taken (Infinity x-21C EMZ 13TR Meiji). All shown images are at the same magnification. The fiber pullout at failure for pure fiber panels are shown in Figures Figure 2 and Figure 3 for OCC, WL, kenaf, and RT, respectively, all pressed at 150 psi.

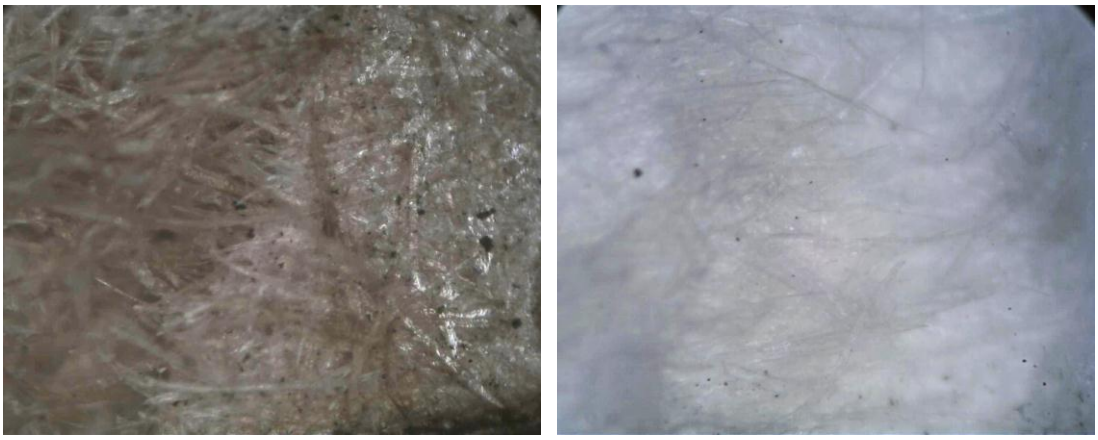

Figure 2: OCC panel (left) and WL panel (right) both pressed at 150 psi, after specimen failure.

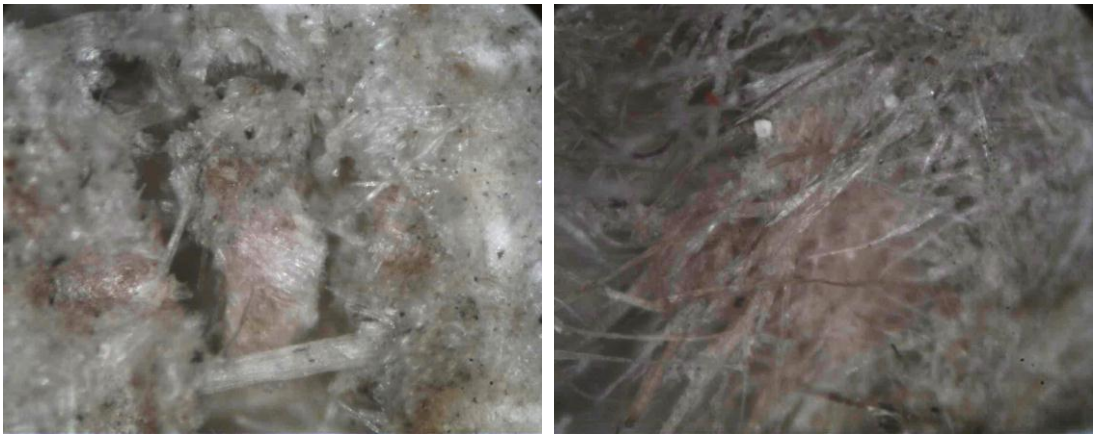

Figure 3: Kenaf panel (left) and RT panel (right) both pressed at 150 psi, after specimen failure.

OCC and RT fibers both appear long and with similar fiber thickness. WL fibers are finer than OCC, while kenaf is much thicker and shorter and appears in the form of larger chunks of material rather than as fibers. Blended fiber compositions are shown in Figure 4 and Figure 5 for 50/50 OCC/WL, 50/50 OCC/Kenaf, and 50/50 OCC/Oat.

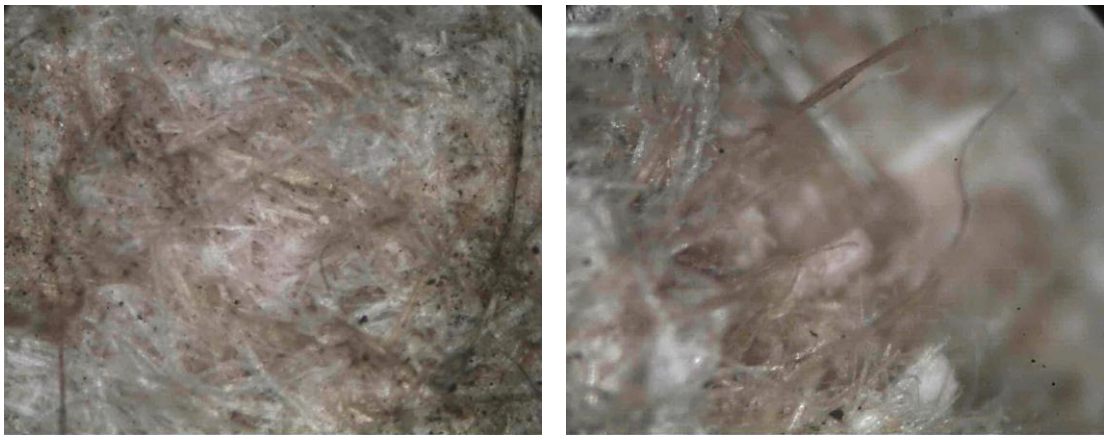

Figure 4: 50/50 OCC/WL panel (left) and 50/50 OCC/Kenaf panel (right) both pressed at 150 psi, shown after specimen failure.

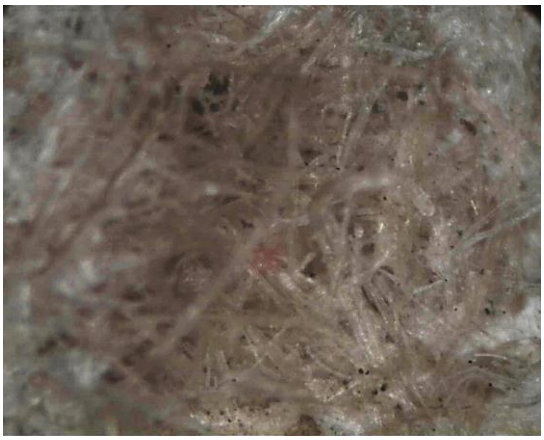

Figure 5: 50/50 OCC/Oat panel at 150 psi.

The average density of each panel type has been measured and this average is used for this study. However, it should be noted that in reality the density profile through the thickness of the panel is non-uniform with the density highest close to each face of the panel, and lower at the center of the panel thickness [19].

3.2 Testing Overview

The primary goals of mechanical testing are the measurement of properties including: including: elastic modulus, yield strength, strain at yielding, ultimate strength, and strain at final failure (ultimate strain). These quantities are determined from the stress vs. strain curve obtained by a tensile test. Tensile strength properties for raw (RA) and resin-coated (HP) panels are compared to assess the effects of adding the resin. In addition, transverse (i.e., panel's through-thickness) shear strengths are measured using a short beam shear test procedure. The numbers of each panel variant tested for each type of test are shown in the test matrices for raw panels (

Table 1) and resin-coated panels (Table 2). A set of resin-coated panels were tested without recorded laser extensometer (strain measurement) data. For these specimens, yield and ultimate strength data were still obtained and are shown in Table 3. In these tables, the term 'Resin %INH' refers to the amount of INH added in the resin mix, inversely proportional to resin viscosity. Based on the manufacturer's specifications mixes with 0%, 25%, and 50% INH have viscosities of 1300, 770, and 475 cPs, respectively, at 74°C.

Table 1: Test matrix for RA (raw) panel specimens

Fiber Blend	*Processing Pressure*	*Resin %INH*	*# Tensile Specimens*	*# Shear (SBS) Specimens*
OCC	50	-	3	3
OCC	150	-	3	3
OCC	250	-	3	3
WL	150	-	3	3
RT	50	-	2	-
RT	100	-	2	-
RT	150	-	3	-
RT	200	-	3	-
Kenaf	150	-	3	-
25/75 OCC/WL	50	-	3	3
25/75 OCC/WL	150	-	3	3
25/75 OCC/WL	250	-	3	3
50/50 OCC/WL	150	-	3	-
50/50 OCC/Kenaf	150	-	3	-
50/50 OCC/Oat	150	-	3	-
75/25 OCC/Kenaf	150	-	3	-
75/25 OCC/Oat	150	-	3	-

Table 2: Test matrix for HP (resin-coated) panel specimens

Fiber Blend	*Processing Pressure*	*Resin %INH*	*# Tensile Specimens*	*# Shear (SBS) Specimens*
OCC	50	0	2	-
OCC	150	0	2	-
OCC	250	0	2	-
OCC	50	50	2	-
OCC	150	50	2	-
OCC	250	50	2	-
WL	150	0	3	-
RT	50	0	3	-
RT	100	0	3	-
RT	150	0	3	-
RT	200	0	3	-
25/75 OCC/WL	50	0	2	-
25/75 OCC/WL	150	0	2	-
25/75 OCC/WL	250	0	2	-

Table 3: Test matrix for HP (resin-coated) specimens missing strain measurement data

Fiber Blend	*Pressure*	*Resin %INH*	*# Tensile Specimens*	*# Shear (SBS) Specimens*
OCC	50	25	3	-
OCC	50	50	3	-
OCC	150	25	3	-
OCC	150	50	3	-
OCC	250	25	3	-
OCC	250	50	3	-
25/75 OCC/WL	50	25	3	-
25/75 OCC/WL	50	50	3	-
25/75 OCC/WL	150	25	3	-
25/75 OCC/WL	150	50	3	-
25/75 OCC/WL	250	25	3	-
25/75 OCC/WL	250	50	3	-

3.3 Resin Infusion

Several parameters, in both panel manufacture and the procedure of adding resin, were studied as potentially affecting the ability of the resin to penetrate more deeply into the panels. While a surface coating of resin improves strength and water resistance, a deeper infusion of resin would ensure that the panels remain water resistant even when cuts are made or holes are drilled.

The factors varied in this study include:

- panel material composition
- density of panel (defined by pressure applied at panel manufacture)
- moisture in panels when resin is applied (as-received content stored in room ambient conditions vs oven dried)
- viscosity of resin mixture (directly related to the %INH added to the resin mix)
- method of resin application (roller vs squeegee)
- curing pressure (air dry vs vacuum bag during cure)

Initial hypotheses suggest that a lower density panel would allow resin to seep further into the panels rather than pooling on the surface. Similarly, a lower viscosity resin would infuse more easily than a highly viscous resin. Moisture in the panel affects the ability of the fibers to bind to the resin. In ambient humidity, water molecules bind to the fibers, blocking the resin from binding to the fibers, whereas if the panel is dried out prior to resin application, the sites will no longer be occupied by ambient moisture.

Drying of the panels was achieved by heating in an oven at 150°C for 0.5 hours. Lastly, applying pressure to the surfaces of the panels as the wet resin cures could help drive the resin into the panels.

The fiberboards are manufactured under differing pressure settings when the wet material is heat-pressed to form panels of varying density. The higher the pressure setting, the more densely the material is pressed together, while lower pressure settings allow the fibers to stay more loosely packed. Panels were manufactured at 50 psi, 150 psi, and 250 psi. While exact density varies by fiber type, the 150 and 250 psi pressures produced panels of roughly 18% and 33% higher density relative to the 50 psi panels, respectively.

For desiccation (drying), the panels were placed in an oven for long enough duration to reach a steady state in mass, since the measured mass changes as the moisture evaporates. To determine how long the panels must be kept in the oven, a study was conducted with mass measured periodically (see Figure 6). From these data, the drying procedure was established as subjecting them to 150°C for 30 min. This timing is specific for the particular panel thickness (~ 2.54 mm) and needs to be established for different thicknesses and perhaps even different ambient humidity states.

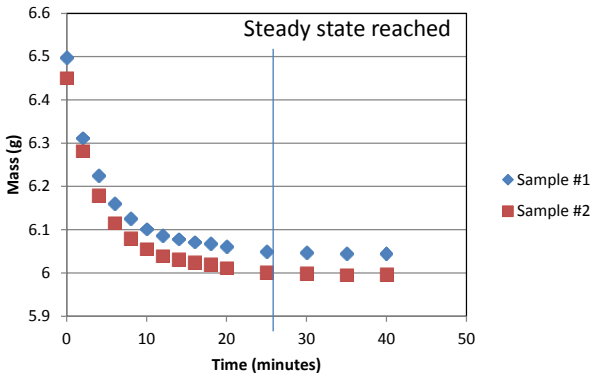

Figure 6: Time history mass data of panels held in oven at 150°C.

To validate the effectiveness of pre-drying, the percent mass increase of resin-coated to raw panels was compared for panels that had been dried in the oven prior to resin application, and panels that were not dried (as-received state, stored at room temperature in ambient moisture conditions). The comparison plot is shown in Figure 7 for samples that had been allowed to air dry and samples cured within a vacuum bag. The percent mass increase was significantly higher for those panels that had been dried prior to resin application, and thus subsequent panels, including test panels listed in Table 2 and Table 3, followed the procedure of all panels being desiccated at 150°C for 30 min. Variation between air dry and vacuum bag cure could be due to inconsistent amounts of resin application, or to differences in how much resin remains pooled on the panel surfaces instead of flowing off when vacuum pressure is applied.

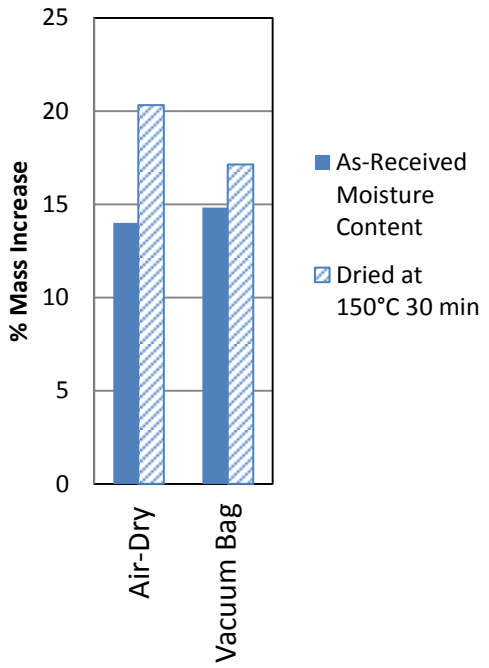

Figure 7: Percent mass increase from raw to resin-coated for room moisture vs dry panels.

The resin selected for this series of testing is Entropy Super Sap® epoxy, a 38% bio-based resin. An optional component, Entropy Super Sap® INH hardener that is used for lowering the viscosity or lengthening the pot life, can be added to the mix in various ratios. According to the manufacturer's specifications, the mixes used in this study at 0% (i.e., no INH added), 25%, and 50% INH weight percent of hardener components have viscosities of 1300, 770, and 475 cPs, respectively, at 23°C. When INH is added to the resin mixture, it is beneficial to post-cure the panels to achieve a more complete degree of resin cure. Thus, panels with an INH resin mix were held at 82°C for 2 hours after curing. This was later reduced to 70°C to avoid potentially softening the resin.

Roller and squeegee application methods were briefly investigated. Roller application correlated to a slightly higher percent increase in mass in both air cured and vacuum pressure panels (Figure 8).

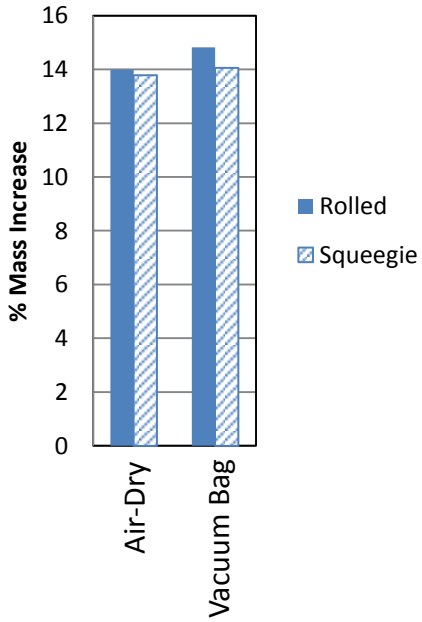

Figure 8: Percent mass increased from raw to resin-coated for roller and squeegie applications.

The differences may be due simply to inconsistent amounts of resin being applied for each method so that the results do not necessarily suggest a deeper resin infusion. Since the differences were not significant and did not suggest deeper infusion, squeegees were used for most HP panels. This allows more accurate tracking of the amount of resin applied to each panel, eliminates the waste from disposable roller-tubes, and also reduces wasted resin which fully saturates the nap of the rollers.

To vary resin infusion driving pressure, half the panels were left on the counter to air cure while the rest were sealed in vacuum bags on flat metal tools, with the vacuum applied at full pressure (-29 inHg) for the duration of the cure (8 hours). Figure 9 shows

data comparing air cured panels to panels cured under vacuum pressure, for panels with roller or squeegie application at ambient moisture, and oven dried with roller application. The vacuum bag did not appear to make a consistently significant improvement, so most panels were allowed to air-dry. The variability could be due to inconsistent amounts of resin being applied, as well as differences in how much resin pools on the panel surface versus flowing off to the side.

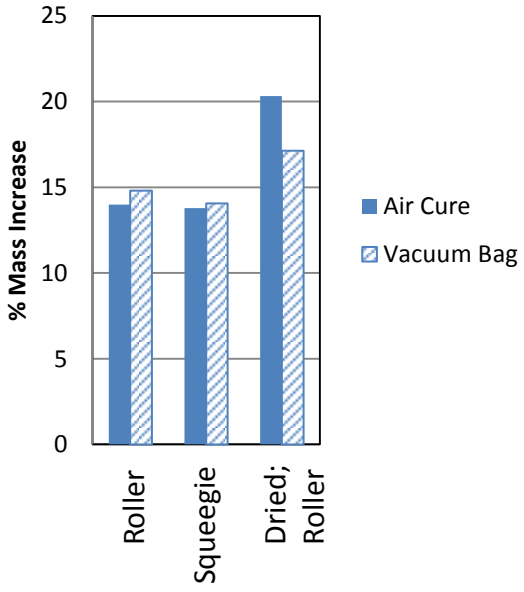

Figure 9: Percent mass increase for air cure and vacuum bag comparison.

Microscope inspection did not suggest significant visual distinction of resin infusion into the panel thickness. Estimation of resin penetration depth was assessed qualitatively by manually indenting at varying through-thickness locations to estimate the hardness. The hardness appeared higher on each face of the resin-coated panels than at the center of the thickness, but the increased hardness did not extend past about a third of the way from each face suggesting resin penetration less than around 0.85 mm. Despite

the lack of full infusion, material properties of surface-only resin-coated panels are still of interest, so the panels were included for tensile testing.

3.4 Tension Tests

From the large panels manufactured as described previously, dogbone test specimens (Figure 10) were laser cut.

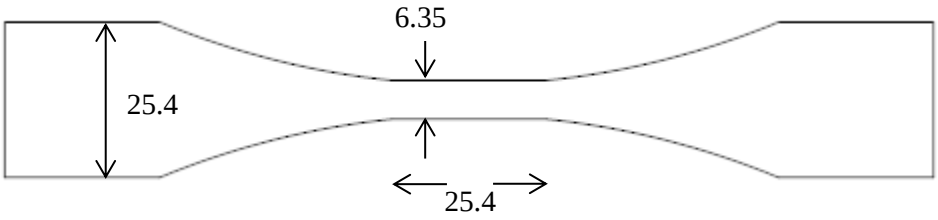

Figure 10: Dogbone test specimen shape, all dimensions in mm.

The wider end tab regions are gripped in the clamps of the test machine. The narrow uniform-width gauge section, where deformation occurs, measures 25.4 mm long by 6.35 mm wide.

Tension testing was conducted using a 100 kN servo-hydraulic material testing machine (MTS 810, MTS Systems Corp., Eden Prairie, MN, USA). The machine was set to displace at a rate of 1 mm/min. Strain was measured by a laser extensometer (Electronic Instrument Research, LE-05, Irwin, PA, USA). Load, actuator displacement, and laser output were recorded. Each test was run until specimen failure.

A MATLAB function (Appendix C: Tensile Data MATLAB Function) extracts key values from the stress-strain curves of each tensile test such as elastic modulus, ultimate strength and ultimate strain. A 0.2% offset yield convention was used to identify yield

stress and yield strain, and values were manually extracted from the intersection point of the stress-strain curve and an offset line parallel to the elastic portion of the curve. These quantities are illustrated on the stress vs. strain curve in Figure 11, where σ is stress, σ_{yield} is the yield stress, $\sigma_{ultimate,}$ is the ultimate stress, ε is strain, ε_{yield} is yield stain, $\varepsilon_{ultimate}$ is ultimate strain, and E is the elastic modulus.

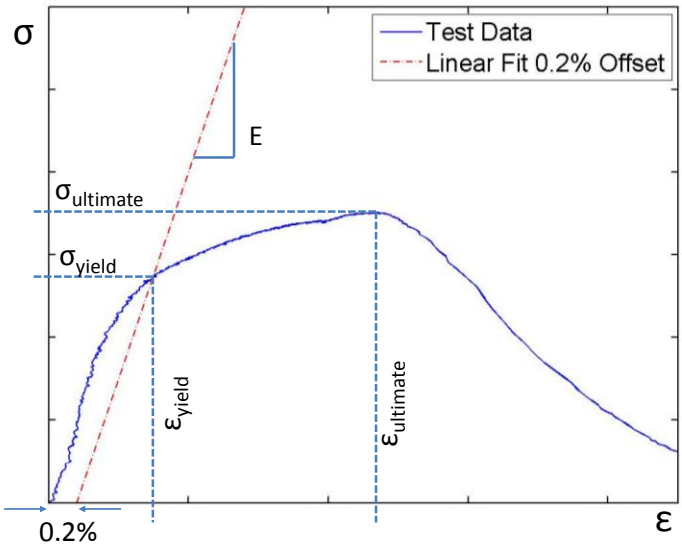

Figure 11: Sample stress-strain curve with key features labeled.

3.5 Short Beam Shear Tests

Short beam shear testing was performed on a subset of panel types. Following the specimen dimensioning guidelines in ASTM D2344 [20] for short beam shear testing, beam specimens were made to be 50.8 mm long, 12.7 mm wide and 8.89 mm thick.. To increase the specimen thickness, the short beam shear specimens were composed of three layers of panels, as shown in Figure 12. The specimens were made by first using a sheet metal shear to cut two inch (50.8 mm) wide strips, then adhering three strips of each

panel variant together using a high strength epoxy resin (PolyEpoxy) to form a panel about 8.89 mm thick. To isolate panel shear strength rather than interlaminar resin strength, an odd number of plies was chosen so that the maximum shear stress, which occurs at the center of the beam height, would coincide with the center of a panel ply rather than in a resin layer. Individual smaller beam samples were then carefully cut with a bandsaw to 12.7 mm width, resulting in an overall 12.7 mm by 50.8 mm by 8.89 mm (thick) geometry. Since the short beam shear testing required a 3-ply thickness of panels, bonded together by resin, and the failure mode was mid-panel where resin would not penetrate, no separate shear testing of surface-only resin-coated panels was done.

Figure 12: Side view of short beam shear test specimen.

Per the ASTM D2344 procedure, bend test fixtures were used in the MTS machine to achieve three-point bending. The total outer roller span length was set to 30.5 mm, and rollers of 3.2 mm diameter. The displacement rate was set to the same rate as tensile testing, 1 mm/min. Load and actuator displacement were recorded. Testing was run until either a significant load drop or visible specimen failure was observed.

The maximum loading experienced was used to compute short-beam shear strength per ASTM D2344 as

$$F^{sbs} = 0.75\frac{P_m}{bh}$$

where F^{sbs} is the short beam shear strength in MPa, P_m is the maximum load during test in N, b is the measured specimen width in mm, and h is the measured specimen thickness in mm. This was obtained assuming a parabolic stress distribution through the panel thickness, such that the maximum shear stress is

$$\tau_{max} = 1.5\frac{s}{a}$$

where τ_{max} is the maximum shear stress experienced, s is the maximum shear force, and a is the cross sectional area. Since the applied load P_m is split across the two supports in a three-point bend test, the maximum shear is half of the applied load,

$$s = 0.5P_m$$

hence the factor of 0.75 in the expression for short beam shear strength.

4 RESULTS & DISCUSSION

A total of 49 raw tensile tests, 69 HP tensile tests, and 21 shear tests were conducted. The data from tension and short beam shear testing of RA panels is compiled in Table 4, with the entry '-' under resin %INH to represent that no resin was used on the panels. Blank cells for shear data represent panel variations that were not tested in shear. Table 5 reports the results of all HP resin panels. Detailed trends are discussed in the following sections, but it is immediately notable that the recycled urban fibers OCC and WL exhibit the highest strengths and that the processing pressure correlates strongly to higher panel strengths and elastic modulus.

Table 6 shows properties for the same fiber type and pressure side-by-side in raw and HP (resin-coated) form, with percent increases to the side and errors below. Initial comparison shows that adding resin consistently improves the strength of the panels.

Table 4: Property compilation for all raw (RA) panels

Fiber	Pressure (psi)	Resin (%INH)	E (GPa)	*E Std Dev*	Yield Strength (MPa)	*Yield Strength Std Dev*	Yield Strain	*Y Strain Std Dev*	Ultimate Strength (Mpa)	*Ult Strength Error*	Ultimate Strain	*Ult Strain Std Dev*	Shear Strength (MPa)	*Shear Str Std Dev*
OCC	50	-	2.63	*0.30*	20.2	*0.62*	0.0097	*0.0009*	23.2	*1.08*	0.0185	*0.0015*	4.29	*0.25*
OCC	150	-	4.46	*1.14*	26.6	*0.78*	0.0083	*0.0020*	32.2	*2.74*	0.0207	*0.0033*	5.90	*0.55*
OCC	250	-	4.87	*0.62*	34.3	*0.71*	0.0091	*0.0010*	40.8	*1.30*	0.0208	*0.0013*	6.73	*0.20*
WL	150	-	4.18	*0.35*	32.2	*1.23*	0.0097	*0.0004*	41.1	*1.79*	0.0361	*0.0004*	5.94	*0.83*
RT	50	-	1.58	*0.11*	11.8	*0.53*	0.0095	*0.0009*	15.6	*0.78*	-0.2622	*0.4912*		
RT	100	-	0.85	*0.81*	11.9	*0.54*	0.0119	*0.0037*	16.4	*0.74*	-0.3161	*0.5923*		
RT	150	-	1.85	*0.47*	13.6	*0.31*	0.0096	*0.0018*	18.9	*0.53*	0.0251	*0.0033*		
RT	200	-	2.21	*0.08*	15.0	*1.72*	0.0088	*0.0006*	21.7	*0.89*	0.0243	*0.0035*		
Kenaf	150	-	4.17	*0.64*	25.1	*1.79*	0.0081	*0.0015*	25.2	*1.98*	0.0082	*0.0018*		
25/75 OCC/WL	50	-	2.99	*0.35*	20.8	*0.81*	0.0090	*0.0005*	24.0	*1.17*	0.0185	*0.0008*	4.21	*0.06*
25/75 OCC/WL	150	-	3.37	*0.16*	26.2	*1.20*	0.0097	*0.0004*	30.8	*1.16*	0.0227	*0.0017*	6.11	*0.28*
25/75 OCC/WL	250	-	4.76	*0.25*	35.4	*2.92*	0.0094	*0.0003*	41.8	*2.32*	0.0213	*0.0024*	7.55	*0.64*
50/50 OCC/WL	150	-	3.58	*0.32*	26.2	*1.54*	0.0093	*0.0003*	31.6	*1.06*	0.0249	*0.0028*		
50/50 OCC/Kenaf	150	-	3.51	*0.33*	28.5	*1.06*	0.0102	*0.0005*	31.4	*0.76*	0.0207	*0.0053*		
50/50 OCC/Oat	150	-	2.31	*0.17*	16.4	*0.70*	0.0358	*0.0459*	19.8	*0.44*	0.0224	*0.0056*		
75/25 OCC/Kenaf	150	-	4.36	*0.44*	33.6	*1.40*	0.0097	*0.0005*	38.5	*1.19*	0.0200	*0.0034*		
75/25 OCC/Oat	150	-	2.97	*0.21*	23.1	*1.27*	0.0098	*0.0002*	29.7	*1.94*	0.0275	*0.0014*		

Table 5: Property compilation for all HP (resin-coated) panels

Fiber	Pressure (psi)	Resin (%INH)	E (GPa)	*E Std Dev*	Yield Strength (MPa)	*Yield Strength Std Dev*	Yield Strain	*Y Strain Std Dev*	Ultimate Strength (Mpa)	*Ult Strength Error*	Ultimate Strain	*Ult Strain Std Dev*	Shear Strength (MPa)	*Shear Str Std Dev*
OCC	50	0	4.52	*1.36*	29.2	*1.54*	0.0088	*0.0024*	34.7	*1.13*	0.0161	*0.0009*		
OCC	150	0	4.18	*0.30*	37.7	*0.17*	0.0110	*0.0007*	43.9	*0.52*	0.0182	*0.0033*		
OCC	250	0	5.41	*0.76*	37.8	*0.95*	0.0091	*0.0012*	43.7	*4.13*	0.0150	*0.0051*		
OCC	50	50	4.29	*0.00*	35.8	*1.52*	0.0104	*0.0004*	46.3	*3.21*	0.0255	*0.0047*		
OCC	150	50	6.44	*1.29*	45.6	*0.93*	0.0093	*0.0016*	58.6	*1.38*	0.0238	*0.0008*		
OCC	250	50	5.74	*0.20*	45.6	*0.27*	0.0100	*0.0003*	54.8	*1.07*	0.0207	*0.0012*		
25/75 OCC/WL	50	0	3.79	*0.56*	29.9	*0.47*	0.0100	*0.0013*	37.7	*0.77*	0.0244	*0.0034*		
25/75 OCC/WL	150	0	5.08	*0.31*	38.8	*0.58*	0.0096	*0.0005*	46.5	*2.13*	0.0216	*0.0034*		
25/75 OCC/WL	250	0	5.15	*0.18*	39.2	*0.16*	0.0096	*0.0003*	47.9	*1.50*	0.0219	*0.0061*		
RT	50	0	3.65	*0.19*	32.0	*1.48*	0.0106	*0.0002*	31.9	*3.71*	0.0112	*0.0025*		
RT	100	0	3.68	*0.20*	30.4	*0.93*	0.0103	*0.0002*	34.4	*1.37*	0.0140	*0.0027*		
RT	150	0	4.22	*0.20*	36.1	*0.74*	0.0106	*0.0006*	43.8	*1.39*	0.0177	*0.0016*		
RT	200	0	4.62	*0.64*	36.7	*0.97*	0.0100	*0.0010*	41.1	*3.28*	0.0134	*0.0019*		
WL	150	0	5.57	*1.71*	47.3	*1.23*	0.0097	*0.0008*	54.9	*3.18*	0.0152	*0.0017*		
OCC	50	25							48.5	*2.63*	0.0081	*0.0009*		
OCC	50	50							54.9	*1.96*	0.0071	*0.0006*		
OCC	150	25							55.8	*1.39*	0.0079	*0.0006*		
OCC	150	50							60.5	*0.77*	0.0071	*0.0002*		
OCC	250	25							49.6	*1.79*	0.0071	*0.0005*		
OCC	250	50							52.9	*4.76*	0.0061	*0.0010*		
25/75 OCC/WL	50	25							53.2	*3.4*	0.0090	*0.0013*		
25/75 OCC/WL	50	50							53.3	*1.2*	0.0099	*0.0004*		
25/75 OCC/WL	150	25							54.7	*1.4*	0.0079	*0.0004*		
25/75 OCC/WL	150	50							59.4	*1.0*	0.0081	*0.0008*		
25/75 OCC/WL	250	25							55.4	*1.6*	0.0072	*0.0009*		
25/75 OCC/WL	250	50							55.6	*2.2*	0.0085	*0.0007*		

Laser extensiometer data not recorded

Table 6: RA to HP property comparison

			E (GPa)			Yield Strength (MPa)			Yield Strain			Ultimate Strength (MPa)			Ultimate Strain		
Fiber	Pressure (psi)	HP Resin (%INH)	RA	HP	% Increase	RA	HP	% Increase	RA	HP	% Increase	RA	HP	% Increase	RA	HP	% Increase
OCC	50	0	2.63	4.52	**71.7**	20.2	29.2	**44.5**	0.010	0.009	**-9.0**	23.2	34.7	**49.8**	0.018	0.016	**-12.8**
		Std Dev.	*0.30*	*1.36*		*0.62*	*1.5*		*0.001*	*0.002*		*1.1*	*1.1*		*0.002*	*0.001*	
OCC	150	0	4.46	4.18	**-6.3**	26.6	37.7	**41.7**	0.008	0.011	**33.0**	32.2	43.9	**36.5**	0.021	0.018	**-12.2**
		Std Dev.	*1.14*	*0.30*		*0.78*	*0.17*		*0.002*	*0.001*		*2.7*	*0.0*		*0.003*	*0.003*	
OCC	250	0	4.87	5.41	**11.1**	34.3	37.8	**10.3**	0.009	0.009	**-0.5**	40.8	43.7	**7.0**	0.021	0.015	**-27.7**
		Std Dev.	*0.62*	*0.76*		*0.71*	*1.0*		*0.001*	*0.001*		*1.3*	*4.1*		*0.001*	*0.005*	
OCC	50	50	2.63	4.29	**63.0**	20.2	35.8	**77.4**	0.010	0.010	**6.8**	23.2	46.3	**99.7**	0.018	0.026	**38.1**
		Std Dev.	*0.30*	*0.004*		*0.62*	*1.5*		*0.001*	*0.0004*		*1.1*	*3.2*		*0.002*	*0.005*	
OCC	150	50	4.46	6.44	**44.3**	26.6	45.6	**71.8**	0.008	0.009	**11.6**	32.2	58.6	**82.0**	0.021	0.024	**14.9**
		Std Dev.	*1.14*	*1.29*		*0.78*	*0.9*		*0.002*	*0.002*		*2.7*	*1.4*		*0.003*	*0.001*	
OCC	250	50	4.87	5.74	**17.8**	34.3	45.6	**33.1**	0.009	0.010	**9.2**	40.8	54.8	**34.3**	0.021	0.021	**-0.5**
		Std Dev.	*0.62*	*0.20*		*0.71*	*0.3*		*0.001*	*0.0003*		*1.3*	*1.1*		*0.001*	*0.001*	
RT	50	0	1.58	3.65	**130.7**	11.8	32.0	**170.2**	0.009	0.011	**11.7**	15.6	31.9	**104.5**	0.021	0.011	**-47.4**
		Std Dev.	*0.11*	*0.19*		*0.53*	*1.5*		*0.001*	*0.0002*		*0.78*	*3.7*		*0.001*	*0.002*	
RT	100	0	0.85	3.68	**332.2**	11.9	30.4	**155.6**	0.012	0.010	**-13.7**	16.4	34.4	**109.6**	0.026	0.014	**-45.8**
		Std Dev.	*0.81*	*0.20*		*0.54*	*0.9*		*0.004*	*0.0002*		*0.74*	*1.4*		*0.001*	*0.003*	
RT	150	0	1.85	4.22	**128.2**	13.6	36.1	**165.9**	0.010	0.011	**9.8**	18.9	43.8	**131.5**	0.025	0.018	**-29.6**
		Std Dev.	*0.47*	*0.20*		*0.31*	*0.7*		*0.002*	*0.001*		*0.53*	*1.4*		*0.003*	*0.002*	
RT	200	0	2.21	4.62	**109.1**	15.0	36.7	**144.2**	0.009	0.010	**14.0**	21.7	41.1	**89.0**	0.024	0.013	**-44.9**
		Std Dev.	*0.08*	*0.64*		*1.7*	*1.0*		*0.001*	*0.001*		*0.89*	*3.3*		*0.003*	*0.002*	
WL	150	0	4.18	5.57	**33.0**	32.2	47.3	**46.9**	0.010	0.010	**-0.4**	41.1	54.9	**33.5**	0.036	0.015	**-58.0**
		Std Dev.	*0.35*	*1.71*		*1.2*	*1.2*		*0.0004*	*0.001*		*1.8*	*3.2*		*0.0004*	*0.002*	
25/75 OCC/WL	50	0	2.99	3.79	**26.8**	20.8	29.9	**43.9**	0.009	0.010	**10.6**	24.0	37.7	**57.4**	0.018	0.024	**32.3**
		Std Dev.	*0.35*	*0.56*		*0.81*	*0.47*		*0.001*	*0.001*		*1.2*	*0.8*		*0.001*	*0.003*	
25/75 OCC/WL	150	0	3.37	5.08	**50.6**	26.2	38.8	**48.1**	0.010	0.010	**-1.9**	30.8	46.5	**51.1**	0.023	0.022	**-4.9**
		Std Dev.	*0.16*	*0.31*		*1.2*	*0.58*		*0.0004*	*0.0005*	**28.1**	*1.2*	*2.1*		*0.002*	*0.003*	
25/75 OCC/WL	250	0	4.76	5.15	**8.3**	35.4	39.2	**10.6**	0.009	0.010	**2.1**	41.8	47.9	**14.7**	0.021	0.022	**3.0**
		Std Dev.	*0.25*	*0.18*		*2.9*	*0.2*		*0.0003*	*0.0003*		*2.3*	*1.5*		*0.002*	*0.006*	

4.1 TENSILE TESTS

Representative stress-strain curves are shown in Figure 13 for OCC at 150 psi, which is a relatively high strength panel. Figure 14 shows the stress-strain curves of kenaf panels at 150 psi, which is a low strength panel exhibiting low ductility. See Appendix B: Stress-Strain Curves for the full set of stress-strain plots from all tensile tests. All plots are shown with the same axis scaling for comparison purposes. The solid line curves represent the stress-strain data of different test specimens, while the dashed lines are linear fits having slope equal to the estimated elastic modulus for each test specimen and are offset by 0.2% strain.

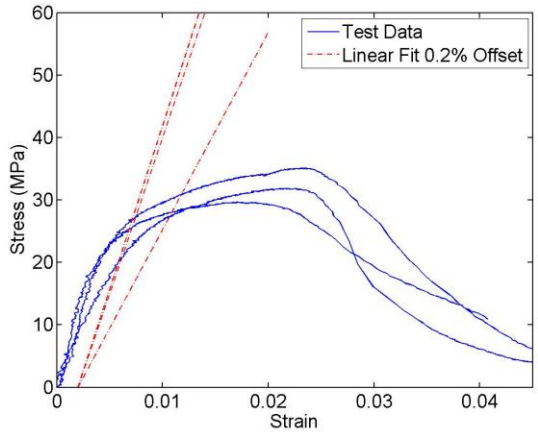

Figure 13: Stress-strain curves for three samples of OCC pressed at 150 psi.

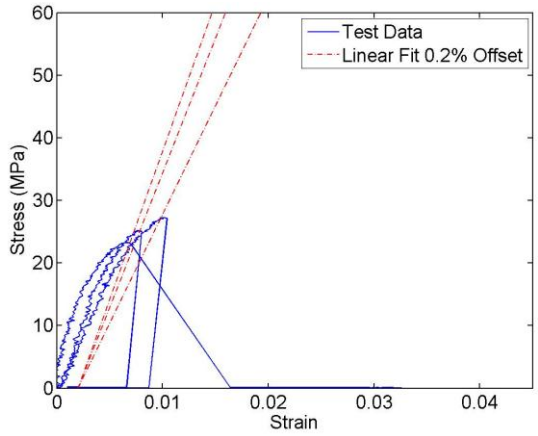

Figure 14: Stress-strain curves for samples of kenaf pressed at 150 psi.

Note the ductility of the OCC panel in comparison to the almost brittle kenaf panel. Most of the panel variations tested showed significant ductility. High levels of ductility may correlate to stronger fiber-fiber bonding, as the ductile yielding region corresponds to when successively more interfiber bonds break and slide apart from each other. A sample test specimen's failure progression over time was captured on video for a WL panel pressed at 150 psi (Figure 15). Separation of some fibers in the panel occurs first on one side, and propagates in a jagged path through the thickness of the panel by

the time final failure occurs. Most of this visible crack formation occurs soon before failure rather than a slow progression over the duration of the test.

Figure 15: Side view of WL, 150 psi specimen undergoing tensile failure. Progression of images captured over 6 seconds.

4.1.1 *Raw Panels*

Key properties are extracted and plotted against each other for the different panel types. For RA (raw) panels, yield and ultimate strengths of each fiber type variation are shown in Figure 16 and Figure 17 for a sense of relative panel strengths. OCC and WL are the strongest individual fibers in both yield and ultimate strengths. For weaker fibers, blending with OCC brings up the overall strength. In the OCC/WL blends the WL, which is strongest in pure form, seems to be limited by the strength of OCC instead of forming intermediate strength panels.

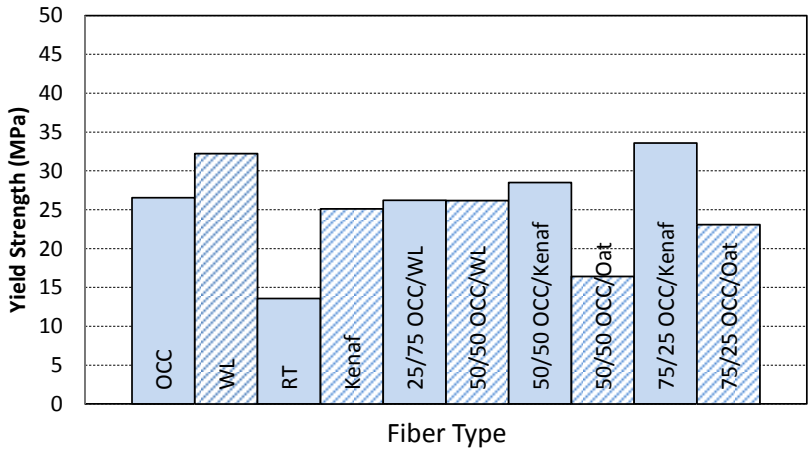

Figure 16: Tensile yield strengths for varying fiber types at 150 psi.

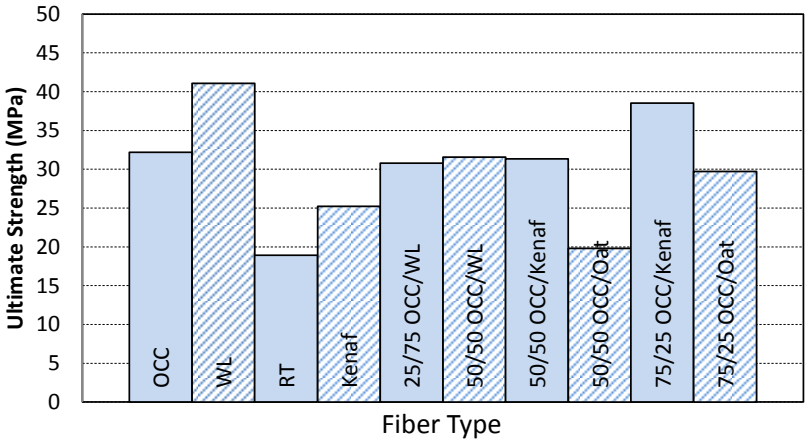

Figure 17: Tensile ultimate strengths for varying fibers at 150 psi.

To further examine the effects of blending different fibers, properties are plotted as a function of percent OCC content. The plot of yield strength as a function of percent OCC is shown for different fiber blends in Figure 18. Increasing content of OCC tends to increase the yield strength for OCC/Kenaf and OCC/Oat blends. However, blended OCC/WL compositions of different ratios all seem to exhibit the strength of the weakest fiber type, instead of demonstrating some intermediate level between pure WL and OCC

properties. This suggests that bonding between the dissimilar OCC and WL fibers is less effective than bonding of fibers of the same type (i.e., WL to WL).

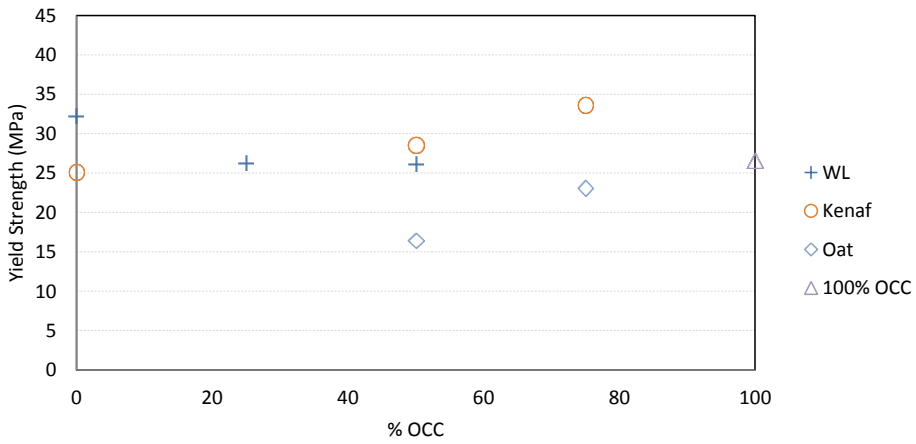

Figure 18: Yield strength for raw panels as a function of percent OCC content.

Ultimate strength as a function of percent OCC is shown in Figure 19, and modulus as a function of percent OCC is shown in Figure 20. Both ultimate strength and elastic modulus demonstrate the same fiber blending trends as observed for yield strength.

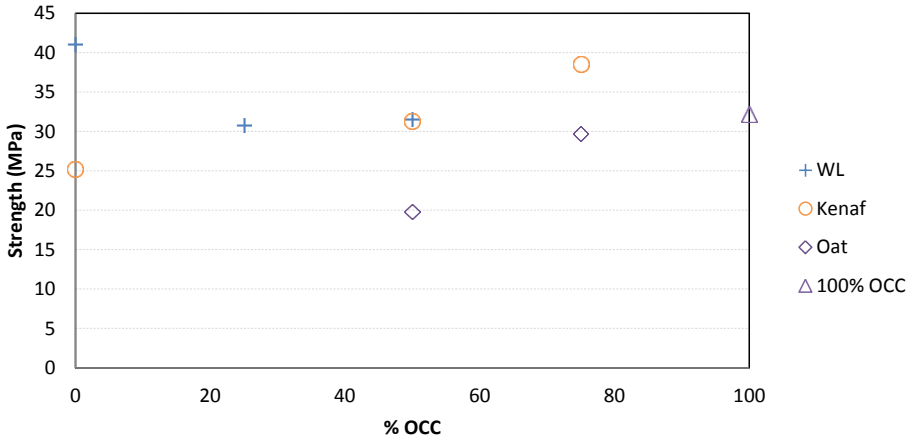

Figure 19: Ultimate strength for raw panels as a function of percent OCC content.

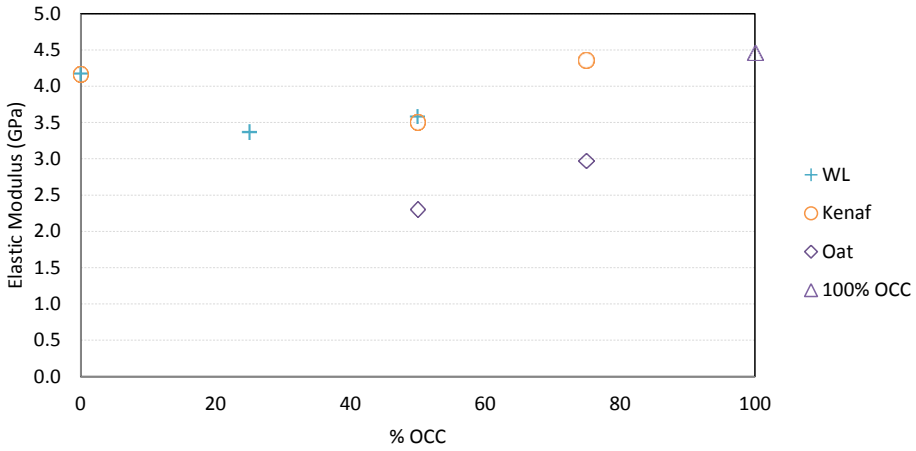

Figure 20: Elastic modulus for raw panels as a function of percent OCC content.

Yield and ultimate strengths as a function of elastic modulus are shown in Figure 21 and Figure 22, respectively. Both are approximately linear, with kenaf and OCC deviating most with relatively low strengths relative to their moduli.

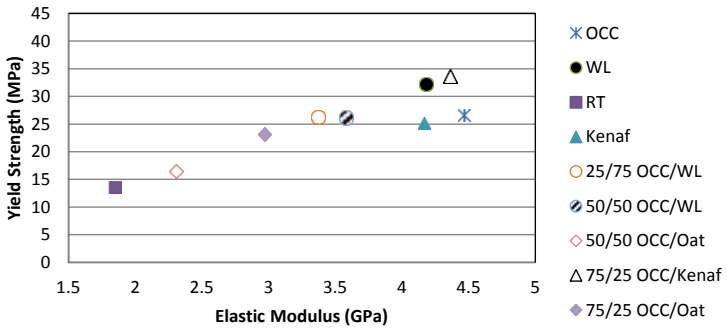

Figure 21: Yield strength vs modulus for raw panels.

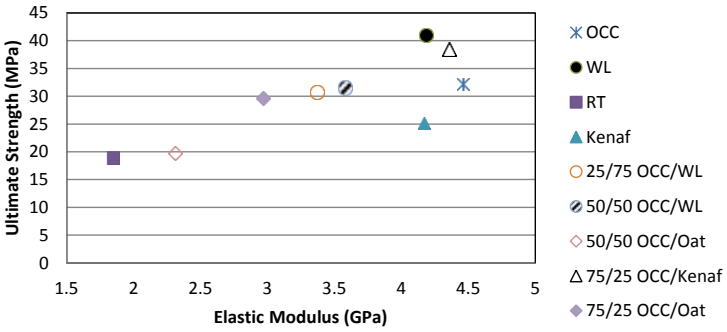

Figure 22: Ultimate strength vs modulus for raw panels.

The density of the various panel types are shown in Table 7.

Table 7: Densities of different panel types.

Fiber Blend	*Processing Pressure*	*Density (g/cm^3)*
OCC	50	0.83
OCC	150	0.98
OCC	250	1.1
WL	150	0.98
RT	50	0.86
RT	100	0.85
RT	150	0.99
RT	200	0.94
Kenaf	150	0.78
25/75 OCC/WL	50	0.86
25/75 OCC/WL	150	0.99
25/75 OCC/WL	250	1.1
50/50 OCC/WL	150	0.91
50/50 OCC/Kenaf	150	0.88
50/50 OCC/Oat	150	0.87
75/25 OCC/Kenaf	150	0.98
75/25 OCC/Oat	150	0.93

Yield strength, ultimate strength, and modulus as a function of panel density are shown in Figure 23, Figure 24, and Figure 25, respectively. Fiber blends for which multiple panel densities were tested were included. Within each fiber type the yield and ultimate strengths tend to increase with increased density. Variations between fiber types could be due to differences in the actual strength of individual fiber-fiber bonds, or in the way fiber pullout occurs after some fiber bonds break. However, the modulus does not show a strong correlation to density.

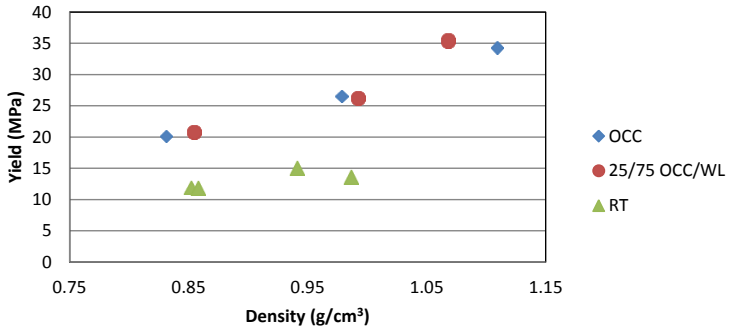

Figure 23: Yield strength as a function of panel density.

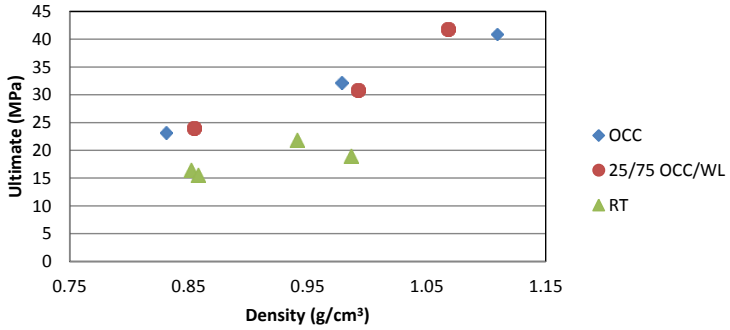

Figure 24: Ultimate strength as a function of panel density.

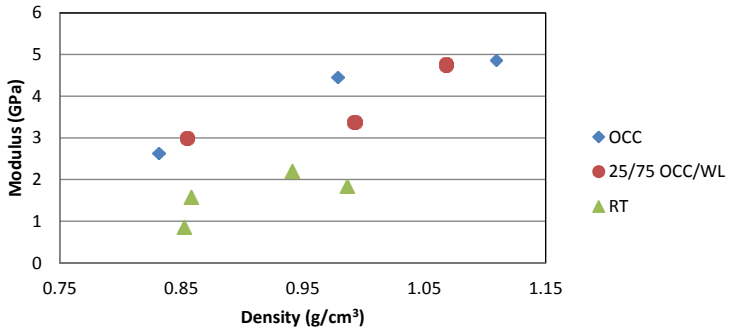

Figure 25: Elastic modulus as a function of panel density.

4.1.2 *HP (Resin-coated) Panels*

Tensile testing results for resin-coated panels are compiled into plots for comparison. Yield and ultimate strengths as a function of modulus is shown in Figure 26 and Figure 27, respectively. There is a slight trend of increasing strength as modulus increases, but the correlation is weaker than for raw panels.

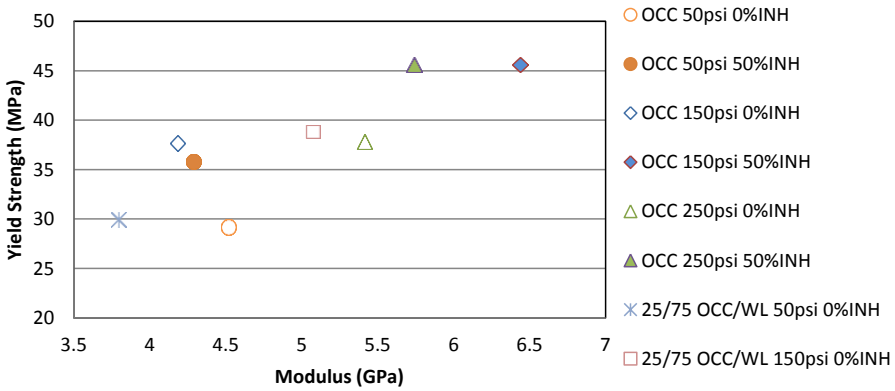

Figure 26: Yield strength as a function of modulus for HP (resin-coated) panels.

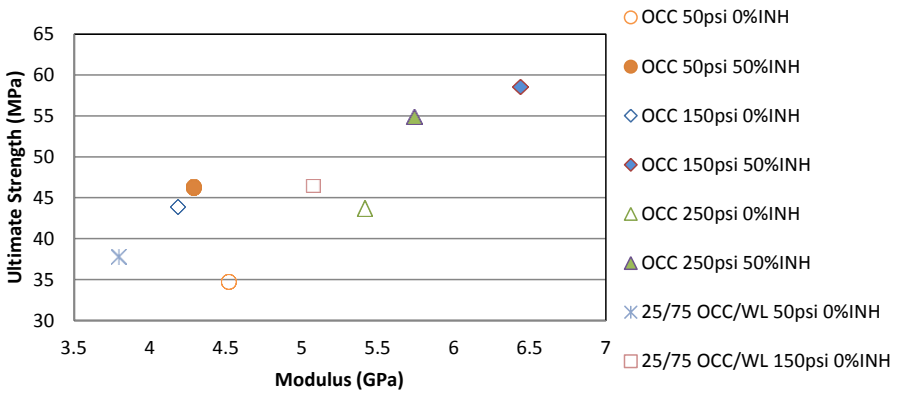

Figure 27: Ultimate strength as a function of modulus for HP (resin-coated) panels.

The strengths and modulus are shown as functions of panel density in Figure 28 and Figure 29, respectively. Note that the uncoated panel density (no resin) is used for these plots rather than the final density after the addition of resin. This is because the goal is to compare the improvement of strength properties for panels of differing initial density when resin is added. The addition of resin resulted in an average of 6% mass increase.

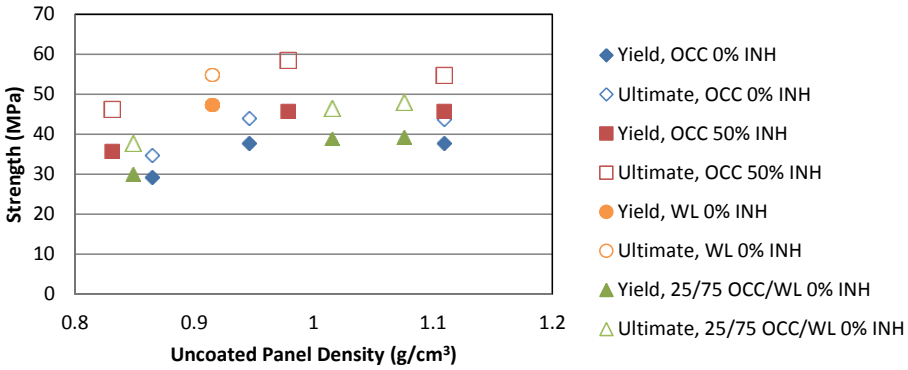

Figure 28: Strength as a function of panel density for HP panels.

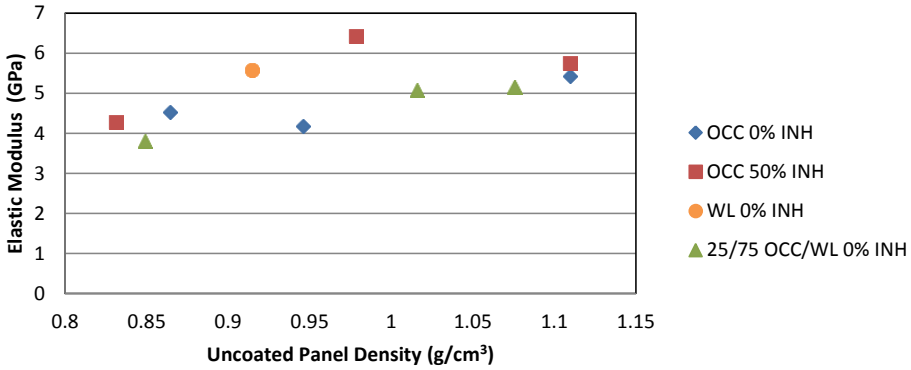

Figure 29: Modulus as a function of panel density for HP panels.

Within each panel type, the lowest panel density exhibits lower strength while the two higher densities have very similar strength values. Strengths increase with density up to a certain point and then levels off, suggesting that other factors beyond the density of bonded fibers limit the maximum strength. Variations in inherent fiber properties such as chemical compositions and physical parameters could play a role. Since the trend applies across the various fiber types, however, it is more likely that the trend arises from the addition of resin to panels of varying densities. It it possible that near each panel face, the applied resin seeps into voids between fibers so that the fibers are held together more strongly. However, the resin is unable to penetrate through the full panel thickness, so even with the addition of resin the weakest panels are still limited by their low initial strengths toward the center of the panel thickness. The total strength for higher density panels levels off potentially because the dense raw panels are inherently stronger, so although the addition of resin brings up the average panel strength the total strength is limited by the strength of the resin-fiber region at each face. It is also possible that the leveling off occurs because the resin is able to penetrate more deeply for lower density

panels, thus the lowest density panel strength increases most while progressively denser panel strengths increase less and less.

To examine the effects of varying resin viscosity, strengths as a function of resin viscosity are shown in Figure 30. For the same panel type, strengths are inversely proportional to the viscosity of resin applied. The same trend was observed for other panel variations as well. This could be due to higher penetration of the resin into the fibers for lower viscosity (e.g., higher %INH addition to thin the resin).

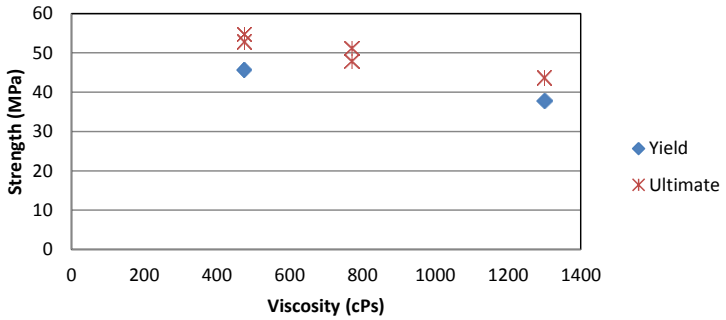

Figure 30: Strengths as a function of resin viscosity for 250 psi OCC panels.

4.1.3 *Raw vs HP (Resin-coated) Panels*

Direct comparison of raw to resin-coated panels provides insights on the effects of applying resin to the panels. It was hypothesized that lower density panels, while less strong in raw form compared to higher density raw panels, have voids that may allow more resin to seep in. Thus, more resin would be absorbed into the body of the panel for a higher overall increase in panel strength. Yield strengths of raw and HP OCC panels are compared in Figure 31. The difference in strength as well as the percent increase in strength from raw to HP panels are shown above the data for each panel density.

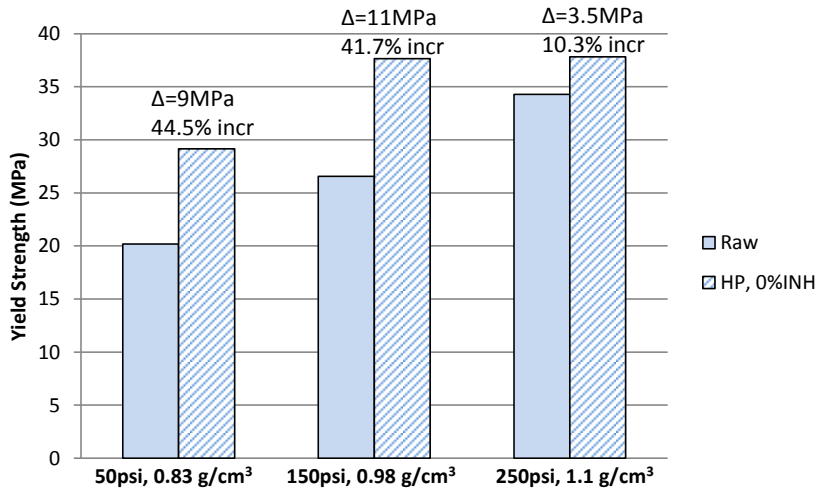

Figure 31: Yield strengths of raw and HP (resin-coated) 0%INH OCC panels at 50, 150, and 250 psi with net increase and percent increase labeled above.

For each density of panel, the addition of resin did increase strength, but the amount of increase from raw to HP is much larger for low density panels than for higher density panels. The lowest density panel strength increased 44.5% from raw to HP, while the highest density panel strength increased only 10.3% from raw to HP. This is likely due to a combination of the higher inherent strength of denser panels and potentially a higher absorption rate of resin into the lower density panels.

The ultimate strengths of raw and HP OCC panels are compared in Figure 32. As with the yield strengths, all panels increased in strength with the addition of resin, but the amount of increase observed dropped off significantly for the highest panel density. The lowest density panel strength increased 49.8% with the addition of resin, whereas the highest density panel strength increased only 7.0% from the addition of resin.

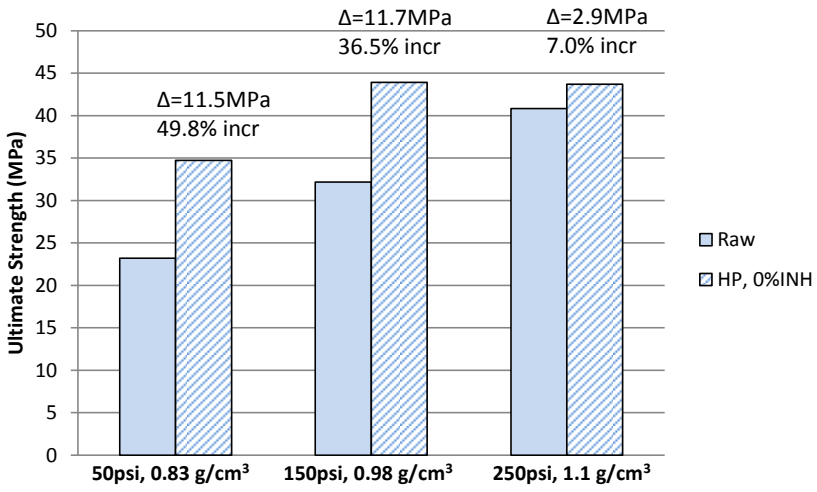

Figure 32: Ultimate strengths of raw and HP (resin-coated) OCC panels at 50, 150, and 250 psi with net increase and percent increase labeled above.

Lower resin viscosity is expected to achieve deeper penetration into the panel, by absorbing more readily into voids between fibers. To study the effects of resin viscosity, strengths of raw and two different resin mixes are shown for OCC panels in Figure 33. Recall that a higher percentage of INH component correlates to a lower viscosity. The data confirms the hypothesis: less viscous resin further improves strength compared to a more viscous resin. For each panel density, note that the percent increase in strength with the addition of 50% INH resin, a low viscosity resin mix, is significantly higher than the percent increase in strength with the addition of 0% INH resin. The same trend of reduced change in strength for high density panels, as described previously from comparison of raw to resin-coated panel strengths, is observed. Though coating the panel with viscous, 0% INH resin only increased the strength of the densest panels by about 7%, switching to 50% INH resin achieved an increase in strength by 34.3% compared to the raw panel. Adding low viscosity resin to the lowest density panel increased the

strength drastically, causing a 99.7% increase in strength. By comparison, adding the 0% INH resin mix with higher viscosity increased the strength of the lowest density panel by 49.8%.

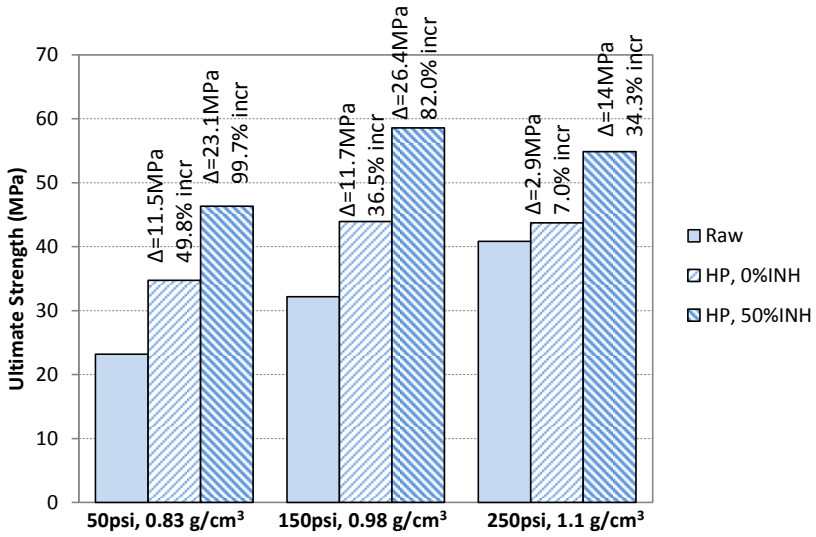

Figure 33: Ultimate strengths of of raw and HP (resin-coated, with 0% INH and 50% INH resin mixes) OCC panels at 50, 150, and 250 psi with net increase and percent increase labeled above.

4.2 Shear Strength

Transverse shear strength values, as determined by short beam shear testing, are shown in Figure 34 for those panel types tested in shear. Shear strengths increase with panel density for each fiber type, a trend that was also observed by the tensile strength tests.

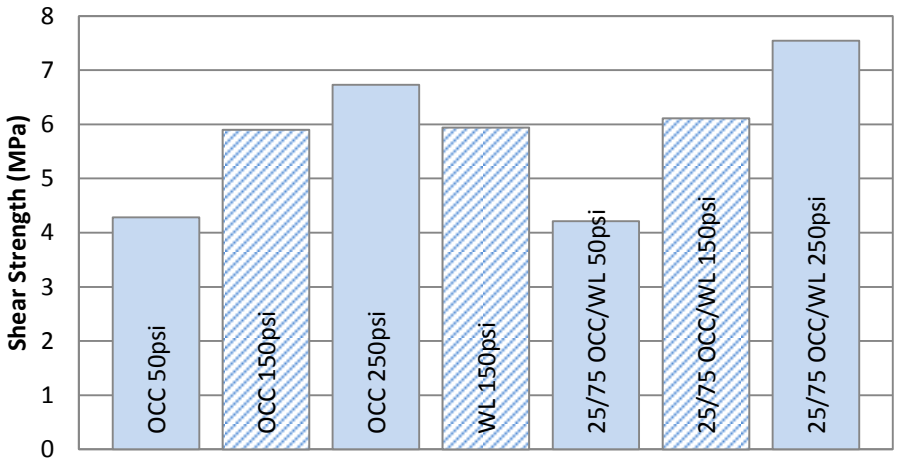

Figure 34: Short beam shear (SBS) strengths of various panel types.

Shear strength is thought to be related to the post-yielding portion of the stress-strain curve as the fibers begin to slide apart and break their bonds prior to ultimate failure. Thus, shear properties are examined in relation to tensile properties in the following plots. Shear strength as a function of density is shown in Figure 35. Shear strength is strongly dependent on and increases roughly linearly with panel density. Density can be seen as the key factor affecting panel shear strength, as higher processing pressure leads to higher density and increased number of bonds between fibers is due to them being compressed more intimately together, and shear strength in turn is highly dependent on fiber bonding. Variation between different fibers is minimal. Note, however, that the fibers tested in shear are all urban fibers which are more processed and refined, leading to lower lignin content and thus stronger fiber-fiber bonds.

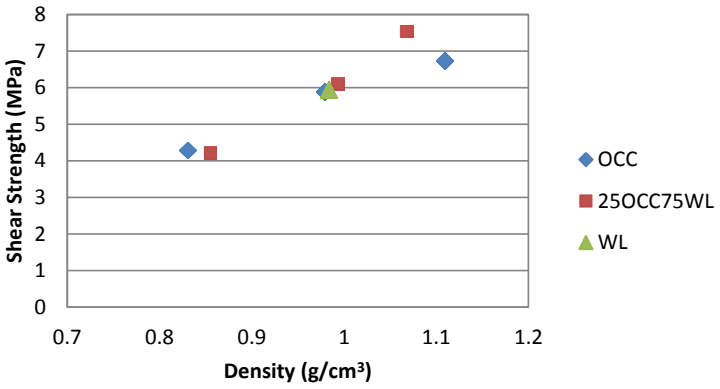

Figure 35: Shear strengths as a function of panel density

The tensile yield strength is shown as a function of shear strength in Figure 36. The yield strength is found to be strongly dependent on and roughly linear with respect to shear strength, again with little variation between fiber type. A linear fit leads shows that the shear strength is about one fifth of yield strength values.

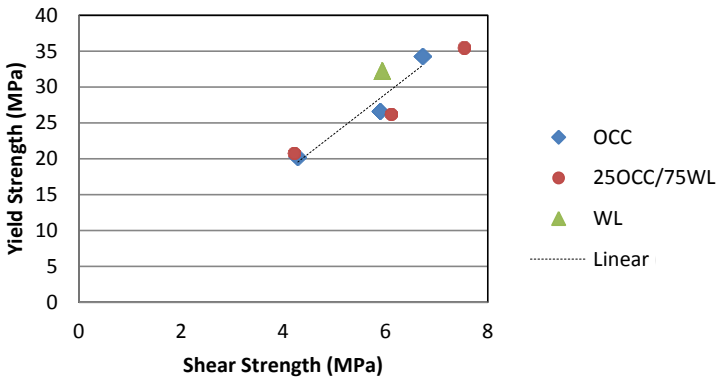

Figure 36: Yield strength as a function of shear strength.

Similarly, ultimate strength is compared to shear strength in Figure 37. The ultimate strength also follows the roughly linear trend, but the deviation is higher, particularly of the wet lap panel.

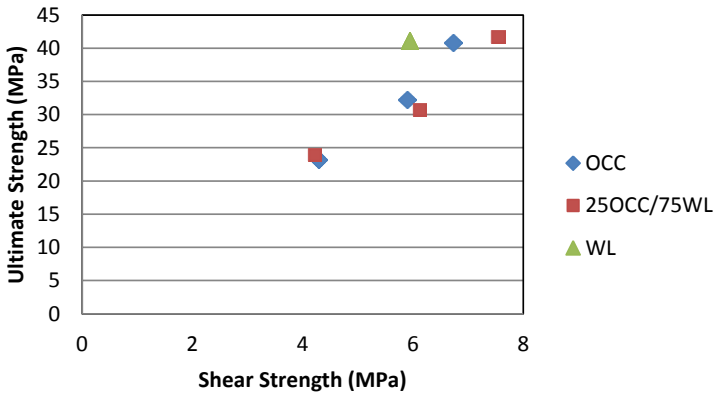

Figure 37: Ultimate strength as a function of shear strength

Elastic modulus as a function of shear strength is shown in Figure 38. The modulus also follows a roughly linearly increasing trend with increasing shear strength.

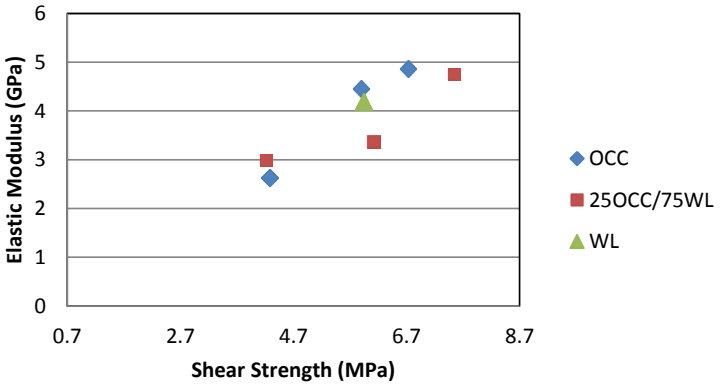

Figure 38: Elastic modulus as a function of shear strength

Yield strain is shown as a function of shear strength in Figure 39. The yield strain appears to be independent of shear strengths. A potential explanation can be rationalized by remembering that strength is directly proportional to the density. With increasing density, the strength is higher by virtue of the tighter packing of fibers into a given volume. While this results in higher modulus and higher yield strength, the strain at

which the panels start to break (damage onset leads to observation of yielding behavior) is not dependent on the packing density of the fibers and is thus nominally the same for the different panel densities. This increase in yield strength with density and invariance of yield strain can be seen by overlaying stress-strain curves for OCC panels of different densities, as shown in Figure 40.

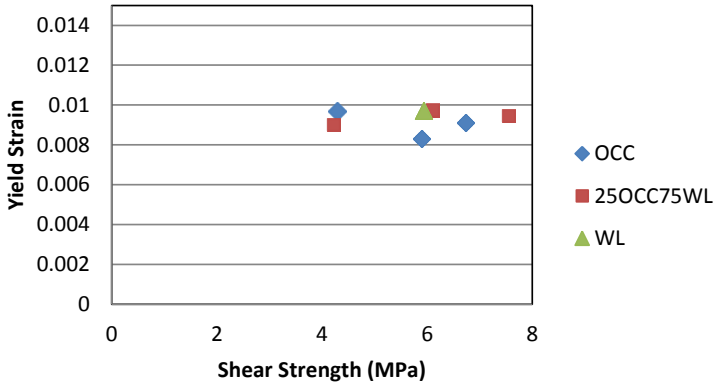

Figure 39: Yield strain as a function of shear strength.

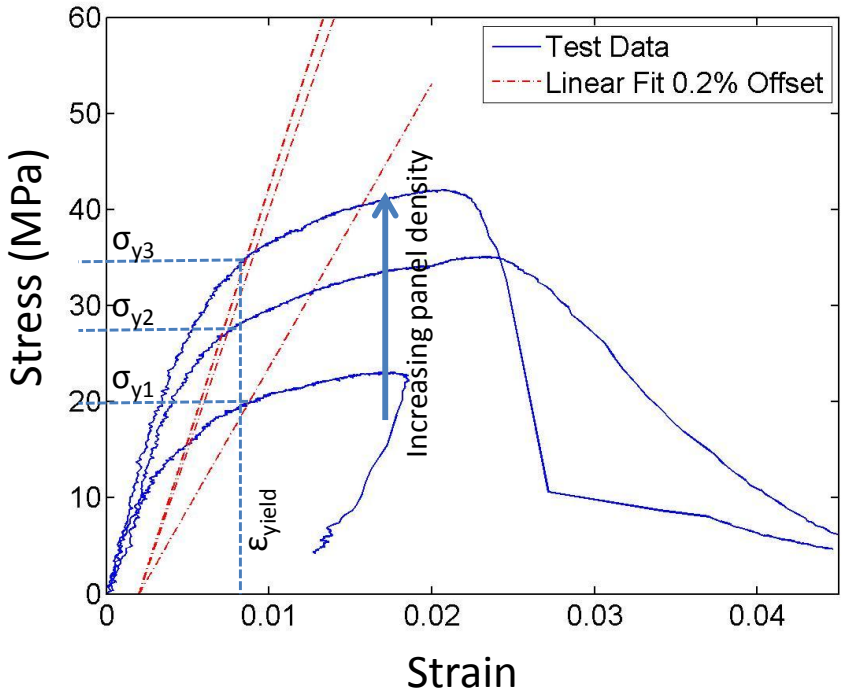

Figure 40: Increasing yield stress and similar yield strain with higher panel densities.

Ultimate strain, shown in Figure 41 as a function of shear strength, has consistent value independent of panel shear strengths with the exception of pure wet lap panels. This could be because ultimate strain is related to the percentage of fiber-fiber bonds broken, thereby permitting the fiber to be stretched to its ultimate level, while shear strength is dependent on the strength of the bonds. The wet lap exhibits much higher ultimate strain despite having a similar yield strain to the other panel variations, suggesting a large ductile yielding region. The shear strength of WL is similar to other panels of the same density, so the effective ductility of a panel is not directly linked to a measure of shear strength. Thus WL seems to be able to withstand significantly more elongation before failure, which could be an indication of crumpled fibers straightening out, less slippage between fibers whose bonds have been broken for delayed failure, or

possibly more interfiber bonds that must be broken before failure. Finally, since the OCC fibers have lower ultimate breaking strain than WL, the OCC fibers in the blend of 25% OCC with 75% WL appear to act like a weakest link and therefore be the limiting factor governing the ultimate strain of the combined material.

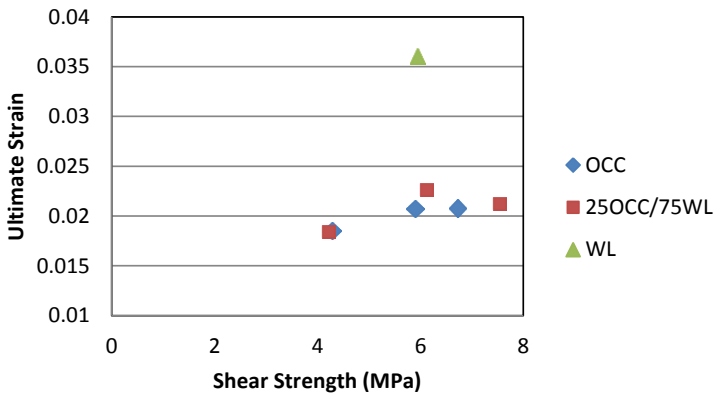

Figure 41: Ultimate strain as a function of shear strength.

Area under the stress-strain curve, a measure of energy dissipated, is shown as a function of shear strength in Figure 42. This dissipated energy density increases roughly linearly with shear strength for the OCC and OCC/WL blend. The pure WL fibers exhibited two times higher dissipated energy than the OCC and OCC/WL blend. This is due to the large ductile region for WL fibers, such that the area encompassed by the curve is much higher.

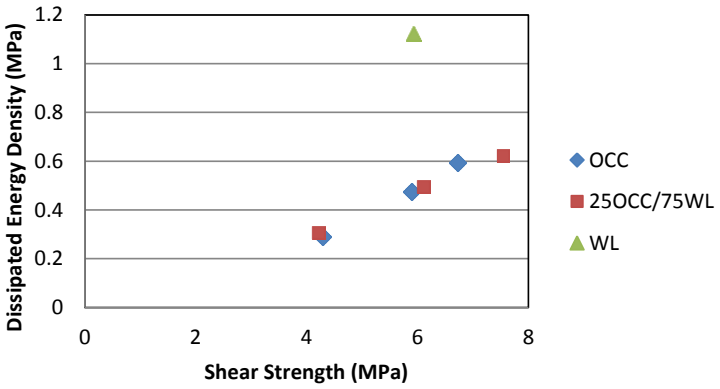

Figure 42: Dissipated energy density (area under the stress strain curve) as a function of shear strength.

4.3 Discussion

Detailed single fiber property measurement and analysis is out of the scope of this project, but the recycled urban fibers, OCC and WL, are known to go through multiple stages of processing and treatment while the agricultural waste fibers are less processed. As discussed in the Literature Review section, more heavily refined fibers generally have lower lignin content, which makes available more cellulose bonding sites and increases the fiber flexibility, allowing fibers to crumple, entangle, and thus bind in more places along the fiber. Oat and kenaf, the agricultural fibers, did exhibit lower strengths than OCC and WL, as expected for stiffer fibers with higher lignin content. A focused fiber-level study of lignin content and fiber geometry could reveal whether the relation between strength and lignin content is dominant or whether other factors (e.g., fiber lengths and geometry) must be studied to accurately predict the performance of new fiber sources.

5 CONCLUSIONS

For the raw (un-coated) panels, OCC and WL exhibit the highest tensile strengths of the fibers tested. Most panels show improved properties when weaker fibers are blended with OCC fibers, but OCC/WL blends of varying ratios are all limited by the weaker of the two fibers. Strengths increase roughly linearly with modulus, for all fiber blends. Strengths also roughly increase with density within each type of fiber blend, but modulus does not appear to correlate so directly. Higher processing pressure helps ensure fibers get pressed together and form more fiber-fiber bonds for stronger panels.

For resin-coated panels, strengths increase with panel density up to a point, then levels off. The addition of resin tends to improve the net panel strength by adding a stronger material coating, but the amount of strength increase is limited by the strength of the resin itself, which has a 65.5 MPa tensile strength and a 3 GPa modulus, or of the resin-fiber bonds. Because the resin does not penetrate through the panel thickness the low density panels are weakened by their low initial strength toward the center of the panel thickness. It is also possible that resin penetrates more effectively into the larger fiber voids of less dense panels, causing a smaller percent increase for progressively higher density panels. With the noted correlation of higher strengths with higher density panels, this diminishing increase would cause the leveling off of final resin-coated oanel strengths. Variation in resin viscosity has the predicted effect, with lower viscosity infusing more effectively into the panel and resulting in stronger resin-coated panels compared to those coated with higher viscosity resin.

The transverse (through-thickness) shear strength of urban fiber panels such as OCC and WL show a clear linearly increasing trend with increasing panel density. The variation between differing fiber types is minimal. Comparing tensile yield strength to shear strength, there is a linear trend, with yield strength consistently about five times larger than shear strength. The strain at yielding was found to be insensitive to the shear strengths. While strengths and modulus correlate directly with the panel density, strains depend on the onset of panel failure rather than the packing density of the fibers. Ultimate strains for OCC and 25/75 OCC/WL blend are also insensitive to shear strengths, but the strain at ultimate failure for WL is much higher. This is due to the long ductile region of WL panel, potentially due to extra length from initially crumpled fibers, higher friction between fibers after bonds break, or a higher number of interfiber bonds to be broken before panel failure. Examining dissipated energy density, WL also deviates from the trend OCC and the OCC/WL blend exhibit, because its ductility encompasses a very high area under the stress-strain curve

When coating the panels with resin, an initial 30 min. drying procedure at 150°C reduced the moisture in the panels, allowing more bonding sites for the resin to bind to the fibers. Other variations in resin application methodology, such as roller and squeegie applications or open air and vacuum bag curing, did not seem to have significant effects on the depth of resin penetration. Lowering the resin viscosity did potentially lead to deeper resin penetration, and was shown to result in higher panel strengths. None of the resin-coated panels appeared to have resin infuse deeper than about a third of the way into the panel thickness, or about 0.85 mm from each free surface.

As noted from the leveling off of strengths for higher panel densities, examining the percent increase from raw to resin-coated panel shows a diminishing increase in strength as panel density increases. The lower density raw panels increase most in strength when a resin layer is added, while the higher density raw panels start out stronger and have less capacity to increase in strength before reaching the resin strength limits.

WORKS CITED

[1] J. F. Hunt and K. Supan, "Mechanical properties for a wet-processed fiberboard made from small-diameter lodgepole pine treetop material," *Forest Products Journal,* vol. 55, no. 5, pp. 82-87, 2005.

[2] J. F. Hunt, A. Ahmed and K. Friedrich, "Effects of fiber processing on properties of fiber and fiberboard made from lodgepole pine treetops," *Forest Products Journal,* vol. 58, no. 6, pp. 82-87, 2008.

[3] A. El-Kassas and A.-H. Mourad, "Novel fibers preparation technique for manufacturing of rice straw based fiberboards and their characterization," *Materials and Design,* vol. 50, no. September 2013, pp. 757-765, 2013.

[4] B. Madsen and H. Lilholt, "Physical and mechanical properties of unidirectional plant fibre composites: an evaluation of the influence of porosity," *Composites Science and Technology,* vol. 63, no. 9, 2003, pp. 1265-1272, 2003.

[5] J. S. Han and J. S. Rowell, "Chemical Composition of Fibers," in *Paper and Composites from Agro-Based Resources*, Boca Raton, FL, CRC Press, Inc., 1997, pp. 85-134.

[6] A. K. Mohanty, M. Misra and L. T. Drzal, Natural Fibers, Bio Polymers, and Bio Composites, Boca Raton, FL: CRC Press, Inc., 2005.

[7] T. G. Rials and M. P. Wolcott, "Physical and mechanical properties of agro-based fibers," in *Paper and Composites from Agro-Based Resources*, Boca Raton, FL, CRC Press, Inc., 1997, pp. 63-82.

[8] E. Frollini, J. Paiva, W. Trindade, I. Tanaka Razera and S. Tita, "Plastics and Composites from Lignophenols," in *Natural Fibers, Plastics and Composites*, Norwell, MA, Kluwer Academic Publishers, 2004, pp. 193-226.

[9] C. Ververis, K. Georghiou, N. Christodoulakis, P. Santas and R. Santas, "Fiber dimensions, lignin and cellulose content of various plant materials and their suitability for paper production," *Industrial Crops and Products,* vol. 19, no. May 2004, pp. 245-254, 2004.

[10] J. F. Hunt and K. Supan, "Binderless Fiberboard: Comparison of fiber from recycled corrugated containers and refined small-diameter whole treetops," *Forest Products Journal,* vol. 56, no. 7/8, pp. 69-74, 2006.

[11] R. Kozlowsky and M. Wladyka-Przybylak, "Uses of Natural Fiber Reinforced Plastics," in *Natural Fibers, Plastics, and Composites,* Norwell, MA, Kluwer

Academic Publishers, 2004, pp. 249-274.

[12] N. Stark, Z. Cai and C. Carll, "Wood-Based Composite Materials-Panel Products-Glued-Laminated Timber, Structural Composite Lumber, and Wood-Nonwood Composite Materials.," *Wood Handbook, Wood as an Engineering Material. General Technical Report FPL-GTR-190.,* pp. 11-4 to 11-15., 2010.

[13] G. Irvine, "The significance of the glass transition of lignin in thermomechanical pulping," *Wood Science and Technology,* vol. 19, no. 05/1985, pp. 139-149, 1985.

[14] O. Suchsland and G. E. Woodson, "Fiberboard Manufacturing Practices in the United States," in *Agriculture Handbook No 640*, United States Department of Agriculture, Forest Service, 1986, p. 25.

[15] D. S. Argyropoulos, "High value lignin derivatives, polymers, and copolymers, and use thereof in thermoplastic, thermoset, and composite applications". U.S. Patent 61/601,181, 21 Feb 2012.

[16] R. E. Mark, "Fibrous Materials," in *Handbook of Physical and Mechanical Testing of Paper and Paperboard*, New York, Marcel Dekker Inc., 1983, pp. 53-77.

[17] A. Bismarck, S. Mishra and T. Lampke, "Plant Fibers as Reinforcement for Green Composites," in *Natural Fibers, Biopolymers, and Biocomposites*, Boca Raton, FL, CRC Press , 2005, pp. 41-60.

[18] R. E. Mark, "Raw Materials," in *Handbook of Physical and Mechanical Testing of Paper and Paperboard*, New York, Marcel Dekker, 1983, pp. 8-30.

[19] J. F. Hunt, J. O'Dell and C. Turk, "Fiberboard bending properties as a function of density, thickness, resin, and moisture content," *Holzforschung*, vol. 62, no. 5 (Sept 2008), pp. 569-576, 2008.

[20] "Standard Test Method for Short-Beam Strength of Polymer Matrix Composite Materials and Their Laminates," *ASTM International*, no. D2344/D2344M, pp. 1-8, 2006.

APPENDIX A: DATA

Table 8: Data from tensile tests of raw (uncoated) panels, for three samples of each panel type. Blank entries were deleted outliers.

Fiber	Pressure (psi)	Density (g/cm^3)	Width (mm)			Thickness (mm)			E (GPa)			Yield Stress (MPa)			Yield Strain			Ultimate Stress (MPa)			Ultimate Strain		
OCC	50	0.83	6.09	6.13	6.15	2.91	2.94	2.97	2.95	2.36	2.59	20.00	20.87	19.66	0.0087	0.0101	0.0103	23.10	22.15	24.31	0.018	0.018	0.020
OCC	150	0.98	6.12	6.13	6.15	2.41	2.37	2.48	5.00	5.23	3.16	26.93	25.67	27.10	0.0072	0.0071	0.0106	35.09	29.64	31.82	0.024	0.017	0.022
OCC	250	1.11	6.19	6.18	6.21	3.29	3.26	3.26	5.29	5.18	4.16	35.00	33.59	34.25	0.0086	0.0085	0.0102	42.05	39.47	40.98	0.021	0.020	0.022
WL	150	0.98	6.28	6.26	6.26	2.68	2.68	2.71	4.30	4.46	3.80	33.34	32.45	30.90	0.0095	0.0095	0.0101	42.63	41.49	39.12	0.036	0.036	0.036
RT	50	0.86	6.17	6.06	6.06	2.64	2.85	2.74		1.67	1.50		11.45	12.20		0.0088	0.0101	16.50	15.14	15.16		0.021	0.022
RT	100	0.85	6.11	6.11	6.12	2.58	2.58	2.63	1.59	0.98		11.52	12.29		0.0093	0.0146		16.65	15.60	17.03	0.025	0.027	
RT	150	0.99	6.10	6.18	6.15	2.66	2.64	2.69	2.37	1.45	1.74	13.54	13.90	13.28	0.0077	0.0100	0.0112	18.78	18.51	19.53	0.021	0.026	0.028
RT	200	0.94	6.16	6.05	6.11	2.32	2.33	2.32	2.23	2.12	2.28	16.35	15.63	13.08	0.0092	0.0090	0.0082	22.11	22.40	20.73	0.024	0.028	0.021
Kenaf	150	0.78	6.02	6.00	6.03	2.42	2.37	2.42	4.30	3.47	4.74	23.29	25.16	26.87	0.0068	0.0079	0.0097	25.16	27.24	23.29	0.008	0.010	0.007
25/75 OCC/WL	50	0.85	6.15	6.15	6.16	3.08	3.13	3.06	3.35	2.96	2.66	21.64	20.70	20.02	0.0085	0.0091	0.0095	25.12	24.01	22.78	0.018	0.019	0.019
25/75 OCC/WL	150	0.99	6.00	6.20	6.16	3.00	2.70	2.80	3.44	3.19	3.48	27.60	25.47	25.56	0.0099	0.0093	0.0100	29.72	30.59	32.02	0.022	0.025	0.022
25/75 OCC/WL	250	1.07	6.19	6.22	6.19	3.18	3.17	3.20	4.68	4.56	5.04	38.27	35.63	32.44	0.0096	0.0096	0.0091	42.93	39.11	43.29	0.024	0.021	0.019
50/50 OCC/WL	150	0.91	6.09	6.09	6.10	2.50	2.47	2.47	3.48	3.94	3.32	27.94	25.30	25.25	0.0091	0.0093	0.0096	31.22	32.74	30.71	0.025	0.022	0.028
50/50 OCC/Kenaf	150	0.88	6.04	6.11	6.05	2.52	2.51	2.51	3.66	3.13	3.73	29.54	28.58	27.43	0.0099	0.0098	0.0108	30.70	31.18	32.19	0.017	0.027	0.018
50/50 OCC/Oat	150	0.87	6.03	6.02	6.04	2.66	2.60	2.58	2.50	2.18	2.25	17.17	16.27	15.80	0.0888	0.0092	0.0092	20.08	19.30	20.03	0.016	0.026	0.025
75/25 OCC/Kenaf	150	0.98	6.07	6.11	6.06	2.44	2.45	2.42	4.83	4.29	3.96	35.16	33.20	32.44	0.0093	0.0097	0.0102	39.88	37.95	37.70	0.017	0.020	0.023
75/25 OCC/Oat	150	0.93	6.07	6.06	6.08	2.56	2.57	2.57	2.77	2.96	3.18	24.55	22.40	22.32	0.0097	0.0096	0.0100	29.29	28.01	31.82	0.027	0.026	0.029

Table 9: Data from tensile testing of HP (resin-coated) panels, for two or three specimens per panel type.

Fiber	Pressure (psi)	% INH	Density (g/cm^3)	Width (mm)			Thick (mm)			E (GPa)			Yield Stress (MPa)			Yield Strain			Ultimate Stress (MPa)			Ultimate Strain		
OCC	50	0	0.83	6.12	6.18		3.16	3.09		5.48	3.56		28.07	30.25		0.007	0.011		35.53	33.93		0.017	0.015	
OCC	150	0	0.98	6.11	6.13		2.59	2.63		3.97	4.39		37.53	37.77		0.011	0.012		43.93	43.93		0.021	0.016	
OCC	250	0	1.11	6.22	6.24		3.63	3.40		5.95	4.87		37.15	38.50		0.008	0.010		40.79	46.63		0.011	0.019	
OCC	50	50	0.83	6.13	6.15		2.97	3.03		4.29	4.29		36.86	34.71		0.011	0.010		48.57	44.04		0.029	0.022	
OCC	150	50	0.98	6.14	6.12		2.39	2.54		5.53	7.35		44.99	46.30		0.008	0.010		57.61	59.56		0.023	0.024	
OCC	250	50	1.11	6.23	6.22		3.37	3.46		5.88	5.60		45.45	45.83		0.010	0.010		55.61	54.09		0.021	0.020	
25/75 OCC/WL	50	0	0.85	6.16	6.15		3.12	3.26		3.40	4.19		29.59	30.25		0.009	0.011		38.28	37.20		0.027	0.022	
25/75 OCC/WL	150	0	0.99	6.03	6.17		3.05	3.04		4.86	5.30		39.23	38.41		0.009	0.010		48.01	45.01		0.024	0.019	
25/75 OCC/WL	250	0	1.07	6.19	6.20		3.27	3.26		5.28	5.02		39.08	39.31		0.009	0.010		46.85	48.97		0.018	0.026	
RT	50	0	0.86	6.08	6.08	6.09	2.60	2.53	2.48	3.73	3.79	3.44	33.00	30.90		0.011	0.010		27.61	34.09	34.00	0.008	0.012	0.013
RT	100	0	0.85	6.13	6.18	6.18	2.70	2.63	2.68	3.69	3.88	3.48	31.37	30.40	29.51	0.010	0.010	0.010	32.98	34.61	35.70	0.013	0.012	0.017
RT	150	0	0.99	6.15	6.15	6.18	2.61	2.61	2.61	4.35	3.99	4.33	36.31	35.27	36.71	0.010	0.010	0.011	43.43	45.40	42.70	0.018	0.019	0.016
RT	200	0	0.94	6.13	6.09	6.10	2.39	2.35	2.35	3.96	5.25	4.65	37.80	36.20	36.04	0.009	0.010	0.011	37.80	41.17	44.35	0.012	0.012	0.016
WL	150	0	0.98	6.14	6.13	6.10	2.76	2.41	2.43	5.93	3.70	7.06	47.95	48.15	45.92	0.009	0.010	0.010	51.28	55.93	57.37	0.015	0.013	0.017

Table 10: Data from short beam shear testing, with three samples of each panel type (a, b, and c).

		Max Force (N)			Width (mm)			Thickness (mm)			Shear Strength (MPa)			Average	Std Dev
Fiber	**Pressure (psi)**	a	b	c	a	b	c	a	b	c	a	b	c		
25/75 OCC/WL	50	751.8	789.0	798.1	14.22	14.42	14.63	9.29	9.90	9.68	4.27	4.15	4.23	**4.21**	*0.06*
	150	1038.5	1057.4	1085.3	14.20	14.03	13.87	9.32	9.39	9.13	5.89	6.02	6.43	**6.11**	*0.28*
	250	1337.7	1367.0	1394.1	14.00	12.60	14.31	10.07	9.83	10.09	7.12	8.28	7.24	**7.55**	*0.64*
OCC	50	724.1	723.3	715.3	14.36	13.51	14.33	8.92	8.81	9.22	4.24	4.56	4.06	**4.29**	*0.25*
	150	869.5	817.2	920.1	14.16	13.99	13.43	7.97	8.08	7.91	5.78	5.42	6.50	**5.90**	*0.55*
	250	1338.7	1261.1	1300.6	14.42	14.35	14.49	10.08	10.11	9.96	6.91	6.52	6.76	**6.73**	*0.20*
RT	50	372.9	325.4	330.7	14.33	14.25	14.32	7.84	7.89	7.66	2.49	2.17	2.26	**2.31**	*0.16*
	100	253.1	256.2	253.4	14.27	13.79	13.83	8.34	8.26	8.21	1.59	1.69	1.67	**1.65**	*0.05*
	200	370.4	347.0	469.6	14.25	14.07	13.90	7.31	7.35	7.06	2.67	2.52	3.59	**2.92**	*0.58*
WL	150	914.3	1094.5	923.7	14.39	14.17	14.37	8.82	8.40	8.73	5.40	6.90	5.52	**5.94**	*0.83*

APPENDIX B: STRESS-STRAIN CURVES

Recall, the solid curves are the test data and dashed lines are linear fits with slopes approximating the modulus of elasticity, E, and are offset by 0.2% strain.

B.1 RAW PANELS

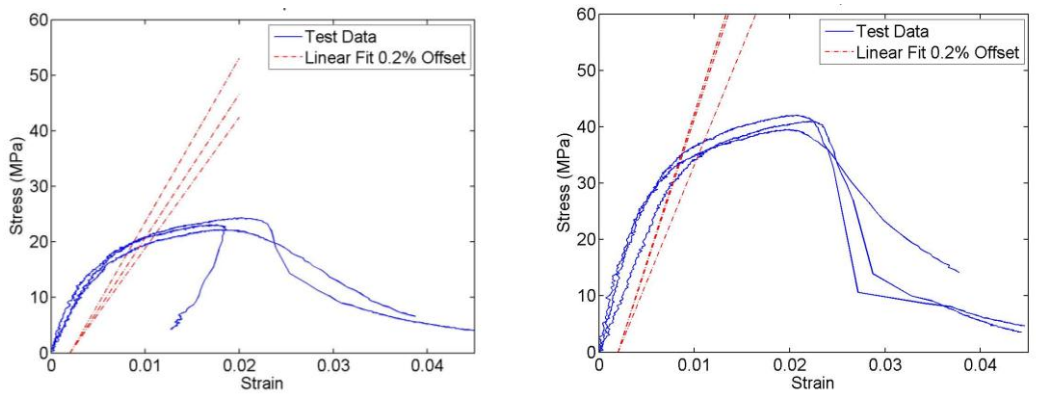

Figure 43: Stress-strain curves for OCC pressed at 50 psi (left) and 250 psi (right).

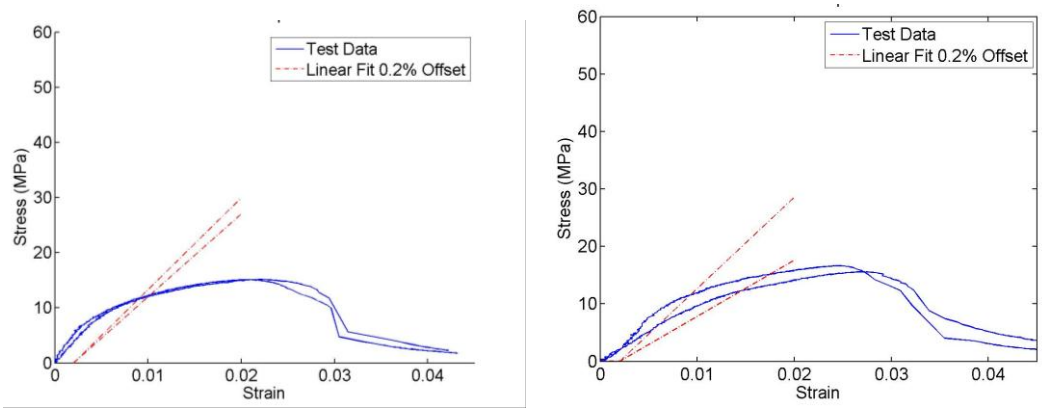

Figure 44: Stress-strain curves for samples of RT pressed at 50 psi (left) and 100 psi (right).

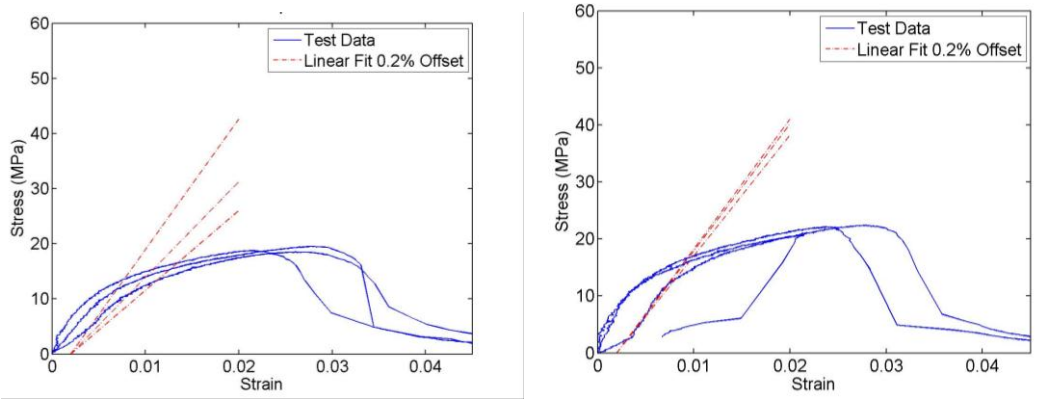

Figure 45: Stress-strain curves for RT pressed at150 psi (left) and 200 psi (right).

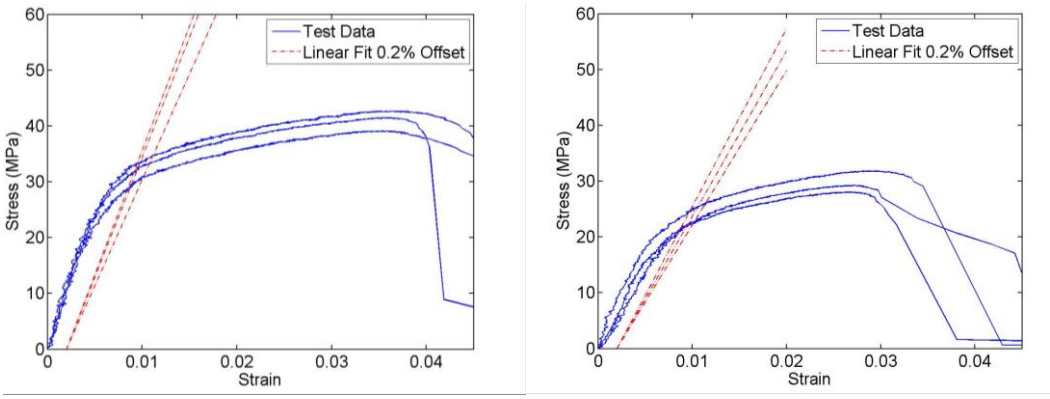

Figure 46: Stress-strain curves for WL pressed at 150 psi (left) and 75/25 OCC/Oat pressed at 150 psi (right).

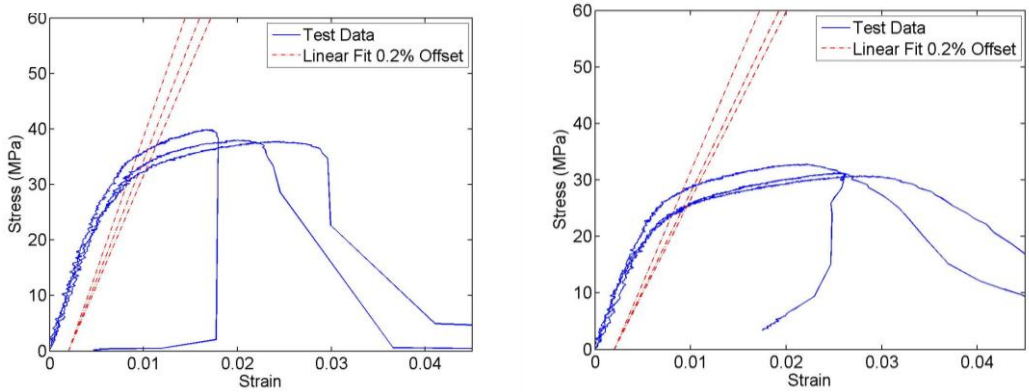

Figure 47: Stress-strain curves for 75/25 OCC/Kenaf pressed at 150 psi (left) and 50/50 OCC/WL pressed at 150 psi (right).

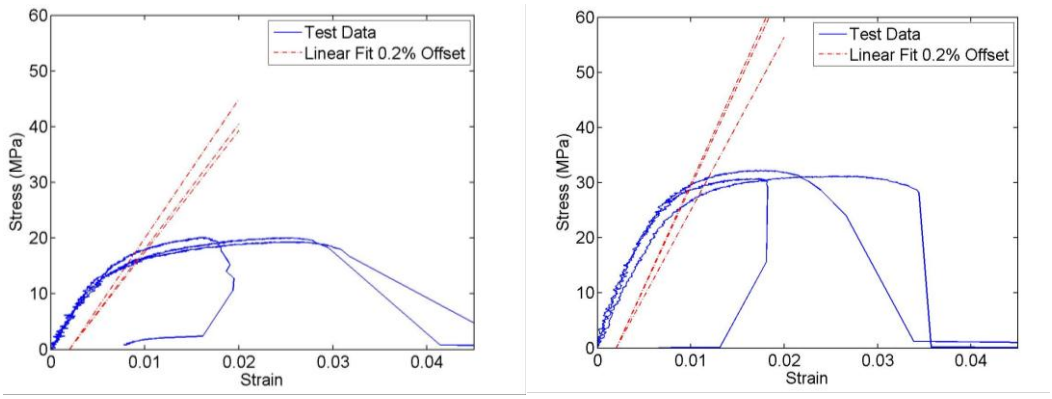

Figure 48: Stress-strain curves for 50/50 OCC/Oat pressed at 150 psi (left) and 50/50 OCC/Kenaf pressed at 150 psi (right).

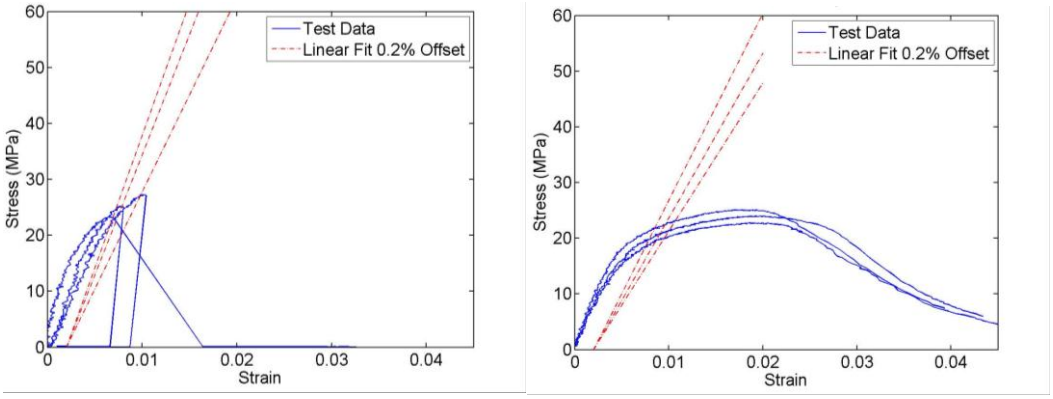

Figure 49: Stress-strain curves for kenaf pressed at 150 psi (left) and 25/75 OCC/WL pressed at 50 psi (right).

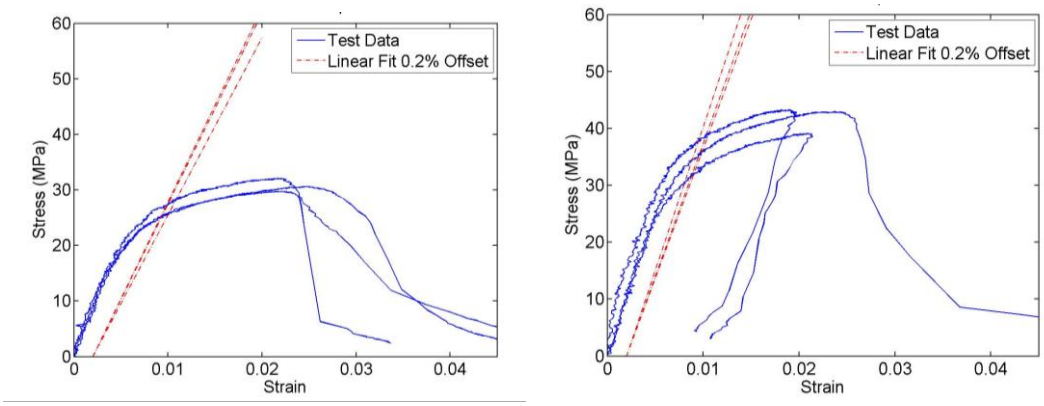

Figure 50: Stress-strain curves for 25/75 OCC/WL pressed at 150 psi (left) and 25/75 OCC/WL pressed at 250 psi (right).

B.2 HP Resin-Coated Panels

Note that trials for which the laser extensiometer did not record were not included since the shape of the stress-strain curve was not represented by the existing data.

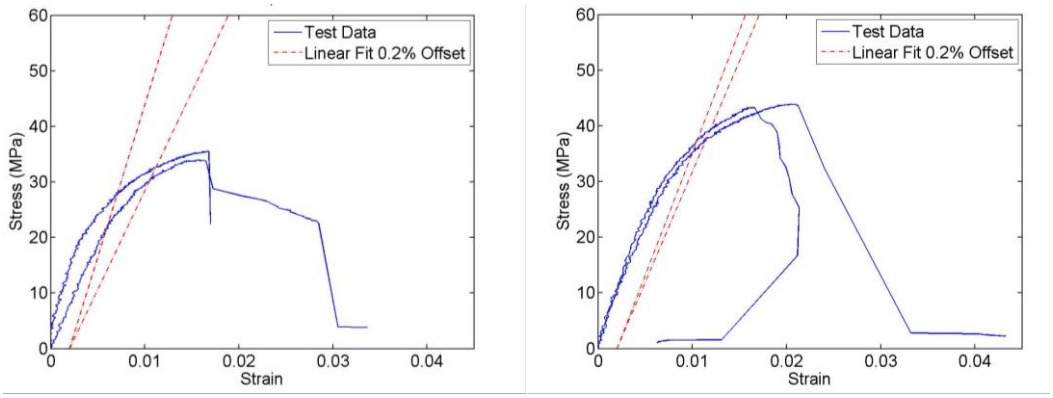

Figure 51: Stress-strain curves for OCC pressed at 50 psi (left) and 150 psi (right), both coated with 0% INH resin.

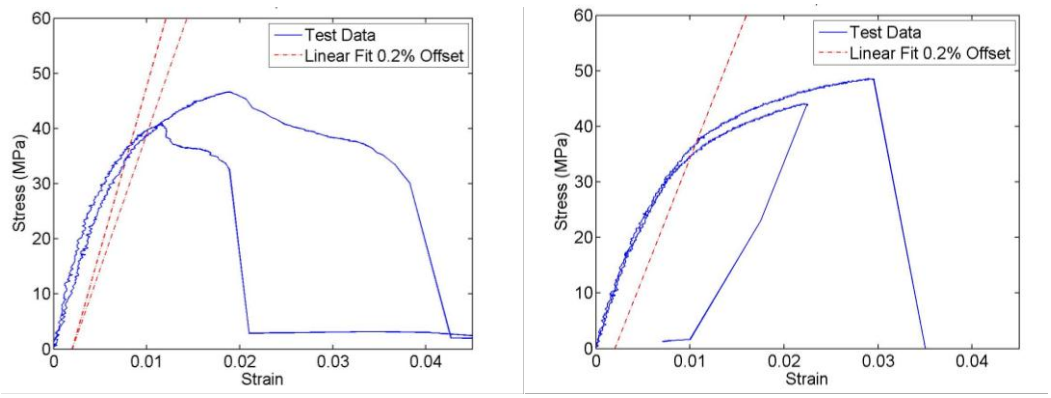

Figure 52: Stress-strain curves for OCC pressed at 250 psi and coated with 0% INH resin (left), and OCC pressed at 50 psi and coated with 50% INH resin (right).

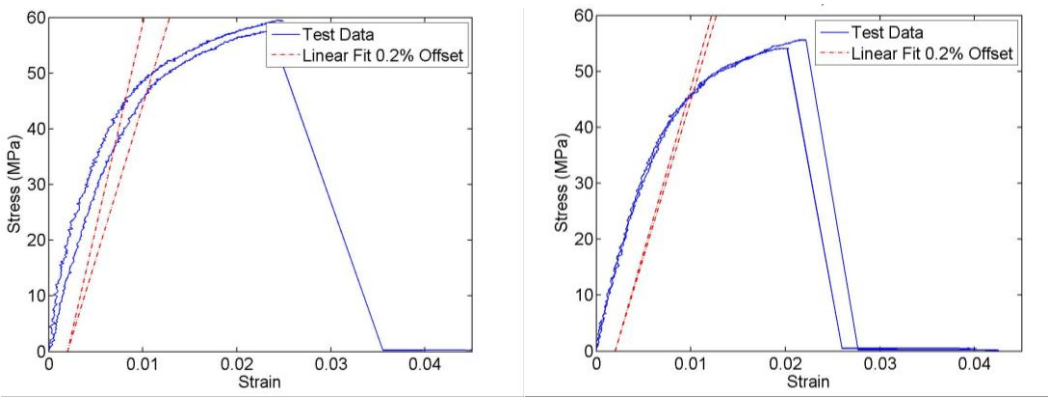

Figure 53: Stress-strain curves for OCC pressed at 150 psi (left) and 250 psi (right), both coated with 50% INH resin

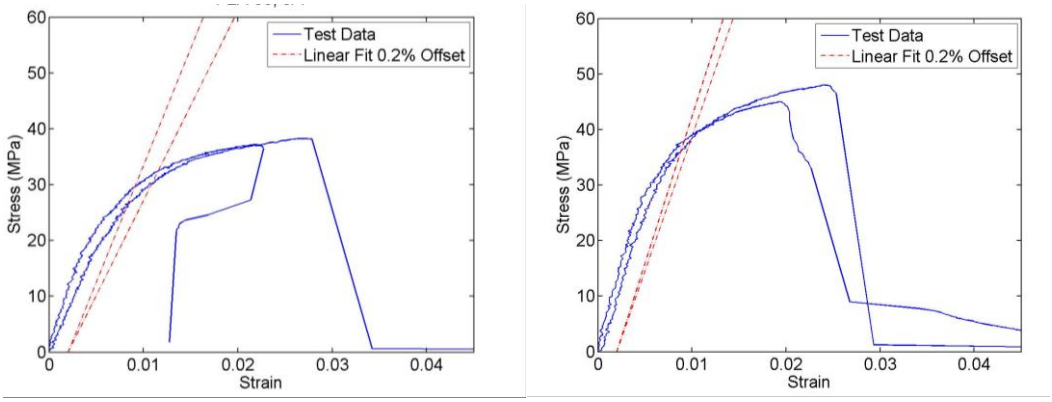

Figure 54: Stress-strain curves for 25/75 OCC/WL pressed at 50 psi (left) and 150 psi (right), both coated with 0% INH resin.

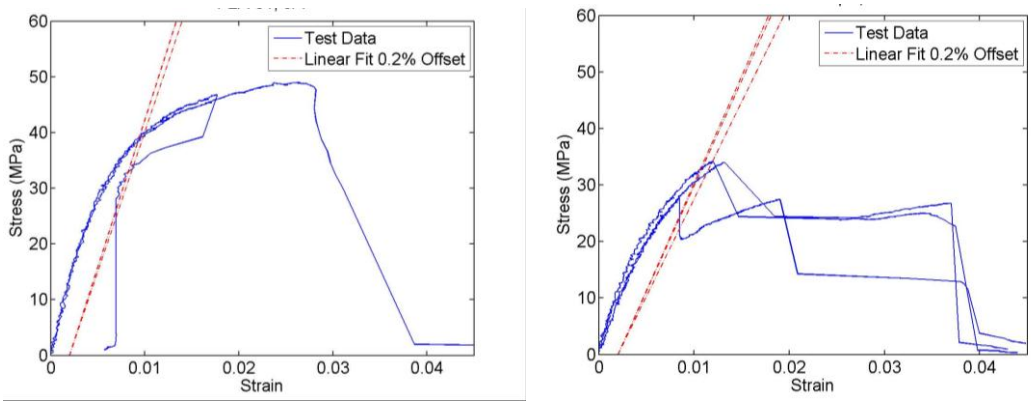

Figure 55: Stress-strain curves for 25/75 OCC/WL pressed at 250 psi and coated with 0% INH resin (left), and RT pressed at 50 psi and coated with resin of 0% INH (right).

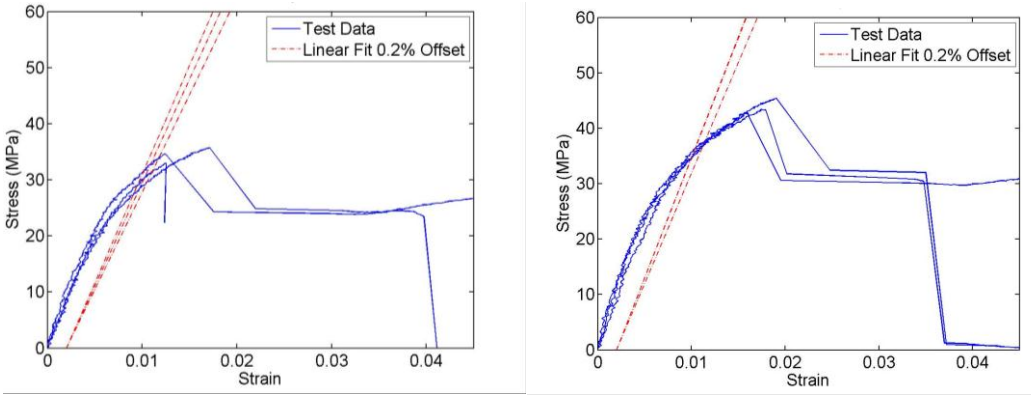

Figure 56: Stress-strain curves for RT pressed at 100 psi (left) and 150 psi (right), both coated with resin of 0% INH.

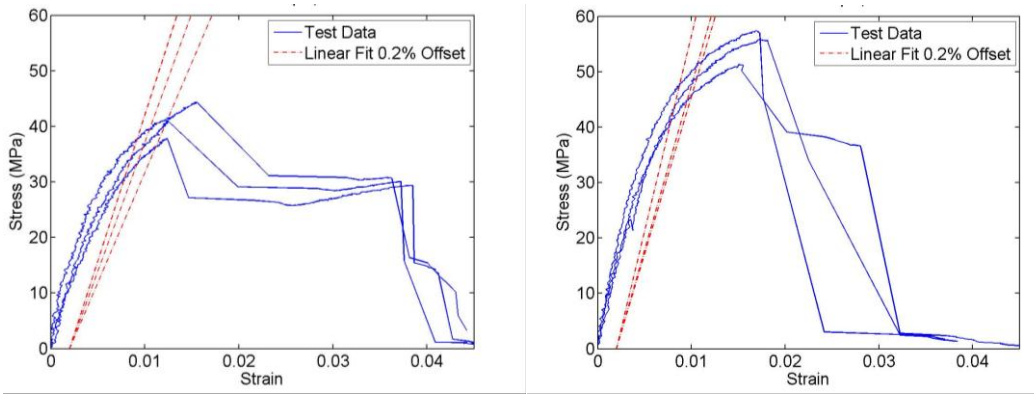

Figure 57: Stress-strain curves for RT pressed at 200 psi and coated with resin of 0% INH (left) and WL pressed at 150 psi and coated with resin of 0% INH (right).

APPENDIX C: TENSILE DATA MATLAB FUNCTION

```
function [stress,strain,E,UltStress,UltStrain] =
ECORtensile(data,dimen)

% Notes:  col1= time (seconds)
% col2= axial displacement (mm)
% col3= axial force (kN)
% col4= strain gage (mm)
% dimen= [width, thickness]

time=data(:,1);
position=data(:,2);
force=data(:,3);
distance=data(:,4);
area=dimen(1)*dimen(2);

[Nrow, ~]=size(data);
%% Stress Strain - Plot
stress=force/area*1000; %MPa, factor of 1000
strain=(distance-distance(1))/distance(1); %dL/Linitial; dL= current
length - initial length
plot(strain,stress,'LineWidth',1.2)
axis([0 0.045 0 60])

%% find slope - Young's Modulus

tstep=time(2)-time(1);
for i=1:Nrow-70
    deriv(i)=(stress(i)-stress(i+50))/(strain(i)-strain(i+50));
end

firstavg=mean(deriv(1:75));
E=firstavg;

%% 0.2% offset yield strength
xintercept=0.002; %to get 0.1% strain offset
x=0:0.00001:0.02;
y=firstavg*(x-xintercept); %y=mx+b
hold on
plot(x,y,'r-.','LineWidth',1.2)
set(gca,'LineWidth',1) %make the axis border thicker
legend('Test Data', 'Linear Fit 0.2% Offset')
set(gca,'FontSize',18)

%% Ultimate Strength
[UltStress,index]=max(stress);
UltStrain=strain(index);
```